Energy Conversion and Management 300 (2024) 117915

Contents lists available at ScienceDirect

Energy Conversion and Management

journal homepage: www.elsevier.com/locate/enconman

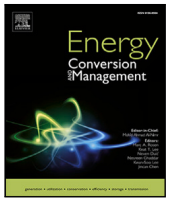

Techno-economic assessment of far-offshore hydrogen-carrying energy vectors off the Iberian Peninsula

Andoni Gonzalez-Arceo [a], Ricardo Blanco-Aguilera [a,*], Joanes Berasategi [a], Manex Martinez-Agirre [a], Abel Martinez [b], Gregorio Iglesias [b,c], Markel Penalba [a,d]

[a] Fluid Mechanics Department, Faculty of Engineering, Mondragon University, Loramendi 4, 20500 Arrasate, Spain
[b] MaREI, Environmental Research Institute & School of Engineering, University College Cork, College Road, Cork, Ireland
[c] University of Plymouth, School of Engineering, Computing & Mathematics, Marine Building, Plymouth, UK
[d] Ikerbasque, Basque Foundation for Science, Euskadi Plaza 5, Bilbao, Spain

ARTICLE INFO

Keywords:
Green hydrogen
H_2-carrying energy vectors
Far-offshore
Floating offshore wind farms
Techno-economics
Levelised cost of energy

ABSTRACT

Green hydrogen (H_2) generation in far-offshore locations is being proposed as an alternative for the decarbonisation of the current fossil fuel-based energy system. However, due to the limited experience and low level of maturity of the technology, an accurate and comprehensive assessment of their technical and economic feasibility is crucial. To this aim, the present paper suggests a holistic numerical model for the techno-economic assessment of diverse H_2-carrying energy vectors, such as gaseous (GH_2) and liquid H_2 (LH_2), and ammonia (NH_3), in far-offshore wind farms. The model includes all the relevant stages, from energy generation, to conversion, transportation, and storage. Hence, the model enables the assessment of broad offshore areas for site selection, sensitivity analyses to identify the most relevant aspects, and optimisation procedures to identify the most suitable H_2-carrying energy vector. The consistency of the model is first verified against the literature and then applied to regions off the Iberian Peninsula and Balearic Islands. Results show that, compared to bathymetry or distance to port, wind resource availability is the most crucial factor to ensure the economic feasibility of the projects. Additionally, for any given site, the full electric alternative turns out to be lower than any H_2-based energy vector. Among the studied H_2-carrying energy vectors, GH_2 is the least expensive one and nearly competitive with electricity, as LH_2 and NH_3 show between two- to three- times greater expenses.

1. Introduction

Achieving a carbon-neutral energy system by 2050 is essential to mitigate the severe consequences of global warming [1–5]. Nevertheless, the transition to a carbon-neutral energy system is a formidable challenge that requires extensive implementation of conventional and emerging renewable energy sources [6]. Wind and solar power will play a significant role, but non-conventional technologies are also crucial. While clean electricity from renewable energies is important, renewable electricity alone cannot drive an effective transition due to its lack of flexibility to match demand in the electric grid and the need for emissions-free thermal energy and fuels. Heat, accounting for nearly 50% of energy use [3,7], and transportation, contributing over 15% of CO_2 emissions [8], require alternative solutions. Direct renewable heat generation and electrification of certain applications can help, but the remaining gap is still significant. In this context, renewable hydrogen (H_2) is expected to play a vital role in the decarbonisation [9]. According to the last Global Hydrogen Review, Europe and Australia are front runners in hydrogen production projects using water electrolysis fed by renewable energy [10]. More specifically, low-emission hydrogen production in Europe could reach close to 5 Mt H_2 by 2030 with Germany and Spain together accounting for 1.4 Mt H_2 [10]. Indeed, the Iberian Peninsula shows a great potential to produce green hydrogen due to the abundance of conventional renewable energy resources [11].

However, generating all the required energy, including electricity, heat and fuels, from renewable sources necessitates a massive increase in renewable energy deployment. In this respect, forecasts indicate that non-conventional renewable energy sources, specifically offshore renewable energies (OREs), will play a crucial role in the energy transition. Nevertheless, a significant portion of the technically available resource, *i.e.* more than 70%, is located in deeper waters (greater than 50 m) and far from the shore (over 90 kilometres) [12]. Therefore, the development of ORE technologies capable of deployment in far-offshore locations spanning hundreds to thousands of kilometres from the shore may become necessary. Floating systems, such as floating offshore wind

* Corresponding author.
E-mail address: rblanco@mondragon.edu (R. Blanco-Aguilera).

https://doi.org/10.1016/j.enconman.2023.117915
Received 15 September 2023; Received in revised form 18 November 2023; Accepted 20 November 2023
Available online 22 November 2023

turbines (FOWTs) and wave energy converters (WECs), have emerged as the most advanced technologies for harnessing energy in such water depths, being FOWTs the most mature technology. Nevertheless, even the floating offshore wind sector is still in a pre-commercial stage, with expectations to reach the commercial stage around 2030 [13]. In fact, the Global Wind Energy Council estimates an installed capacity of 10.9 GW by 2030 [13], while Det Norske Veritas (DNV) estimates that 15% of all the offshore wind energy will be generated by FOWTs, contributing 264 GW to by 2050 [14]. In addition to the increase in FOWT size and power, technological innovations are expected to extend the range of technically and economically viable water depths, enabling the installation of FOWTs in waters of up to 1000 m [15]. These innovations would enable the exploitation of far-offshore locations where the resource is more consistent and powerful.

The delivery of energy from far-offshore ORE farms to end users also poses a significant challenge, as connecting to national electricity grids through conventional electrical cables becomes economically unfeasible [15]. High-voltage alternating current (HVAC) or direct current (HVDC) cables are not be technically viable in this context. To overcome this challenge, the concept of generating green H_2 in far-offshore farms has emerged as an interesting solution. Many energy vectors have been proposed in the literature to transport the far-offshore-generated H_2, which can be produced using desalinated sea water and electricity. Some of these vectors, such as pure hydrogen in either gaseous (GH_2) or liquid (LH_2) form, and ammonia (NH_3), can be produced on site with relatively mature technologies. Others would depend on carbon capture, such as synthetic natural gas (mainly composed of methane), methanol [16] and pure methane [17]. Finally, Liquid Organic Hydrogen Carriers (LOHC) would need a carrier molecule to be brought back from the shore [18,19]. Upon reaching the shore, the H_2 can be unloaded into a H_2 terminal and then distributed to end users through existing pipelines. Energy outlooks estimate that off-grid H_2 generation could constitute a significant 15% share of offshore power generation by 2050 [12].

Given incipient nature and low-maturity of this kind of projects, it is crucial to develop tools to evaluate their feasibility. To this end, the techno-economic analysis is essential and, specifically, the Levelised Cost of Energy (LCOE) has emerged as a fundamental metric to compare different power generation technologies [20–22]. The LCOE quantifies the cost of electricity production over the lifetime of any energy project [23]. Indeed, there already exist various LCOE-based studies for both bottom-fixed offshore wind [24–27] and FOWTs [15,27–30]. These studies have shown that the cost of energy for offshore wind has experienced a great reduction in recent years, although it is still far from conventional renewable energy sources, such as solar, biomass and onshore wind. Additionally, modelling the energy generation taking into account the variability of the wind resource, both temporally and spatially, instead of using average wind speeds, has been demonstrated fundamental for an accurate assessment [15].

Regarding offshore-generated H_2 technologies, the academic literature has paid little attention until relatively recently. Furthermore, the vast majority of studies present generic techno-economic assessment studies where either the ORE generation part [31], the hydrogen generation part [32], or both aspects are excessively simplified [18,33–41]. Considering these limitations, the following section provides an overview of the most comprehensive and up-to-date studies, outlining their main assumptions and identifying any gaps.

Jiang et al. [31] optimises the electrolyser capacity with a model that considers all stages from wind energy generation to H_2 production and transport using vessels. The electrolyser model includes degradation and replacement costs, and dynamically adapts the efficiency based on the instantaneous wind farm power output. However, the wind speed signal is generated following a Weibull distribution, and does not use real wind speed data. In addition, the study only examines a single distance from shore and transport alternative.

Saenz-Aguirre et al. [32] ignores the dynamics of the electrolyser considering a constant conversion rate of 4.2 kWh/Nm^3 to focus on the ORE generation part. The wave and wind energy generation models are also simplified, using a power matrix of individual WECs and an onshore-based wind turbine power curve, respectively. Additionally, the wave/wind resource is modelled as a sinusoidal signal. Lastly, the study completely neglects transport to shore.

In contrast, Franco et al. [18] compares up to seven different energy transport options for different scenarios and parameters. The paper studies the effect of future technology development scenarios, policies, the distance to shore and the wind farm capacity factor. However, the study employs a generic wind farm and does not consider real location data or dynamic effects.

Dinh et al. [33] develops a geospatial model that integrates real location data, including proximity to available harbours, water depth, distance and wind resource, and carries out an assessment study off the Irish coast. However, this work only includes H_2 pipelines as a transport option, neglecting any other alternative. Furthermore, the energy production is estimated based on probabilistic distribution wind speed data at each location, instead of using real time series data.

Giampieri et al. [34] takes into account several transport alternatives, distances to shore and technology development scenarios. However, all calculations are computed based upon wind data for the same location and the same wind farm characteristics, with distance variations affecting only the cost of energy, but not the production.

Finally, Kim et al. [35] presents a comprehensive comparative economic analysis that evaluates the feasibility of offshore wind turbines to supply the onshore green hydrogen demand. The study examines the impact of wind speed, the number of turbines and offshore distance on hydrogen production. It is important to note that the analysis only considers gaseous hydrogen, excluding other potential carriers such as liquid hydrogen or ammonia from the scope of the study.

Based on the literature review, a comprehensive techno-economic evaluation of far-offshore green H_2-carrying vectors should include (i) realistic wind resource data for accurate energy generation estimation, (ii) realistic port locations and vessel characteristics to estimate the transport cost, (iii) dynamic effects resulting from the variability in the wind resource, (iv) different H_2-based energy vectors and transportation alternatives, and (v) losses in the different conversion stages from electricity to each H_2-based vector. Although all reviewed studies consider some of these fundamental aspects individually, to the best of authors' knowledge, none of the studies incorporates and combines all of them. Hence, to address the gaps identified in the literature, this paper aims to develop a holistic techno-economic model for the assessment of far-offshore H_2-carrying energy vectors that combines all the previously listed fundamental considerations in a single framework. In addition, the analysis is carried out for a wide area off the Iberian Peninsula, which can also be considered as a novelty of the present study.

Consequently, the proposed integral techno-economic framework has the capability to (i) assess the feasibility of offshore H_2 production for a broad region, (ii) identify the optimal locations for each H_2-based energy vector, (iii) identify and evaluate the most relevant aspects for H_2-based far-offshore projects, and (iv) determine the best alternative for each location.

The present paper is structured as follows. After this introduction (Section 1), the techno-economic model is defined in Section 2, including both energy and integrated cost submodels. Subsequently, Section 3 presents the methodology followed for the development of the techno-economic numerical framework and describes the case study analysed in the present paper. In Section 4, results are presented, first verifying the developed framework against literature data, and, then, highlighting the main outcomes of the simulations. Finally, Section 5 draws the main conclusions of the study.

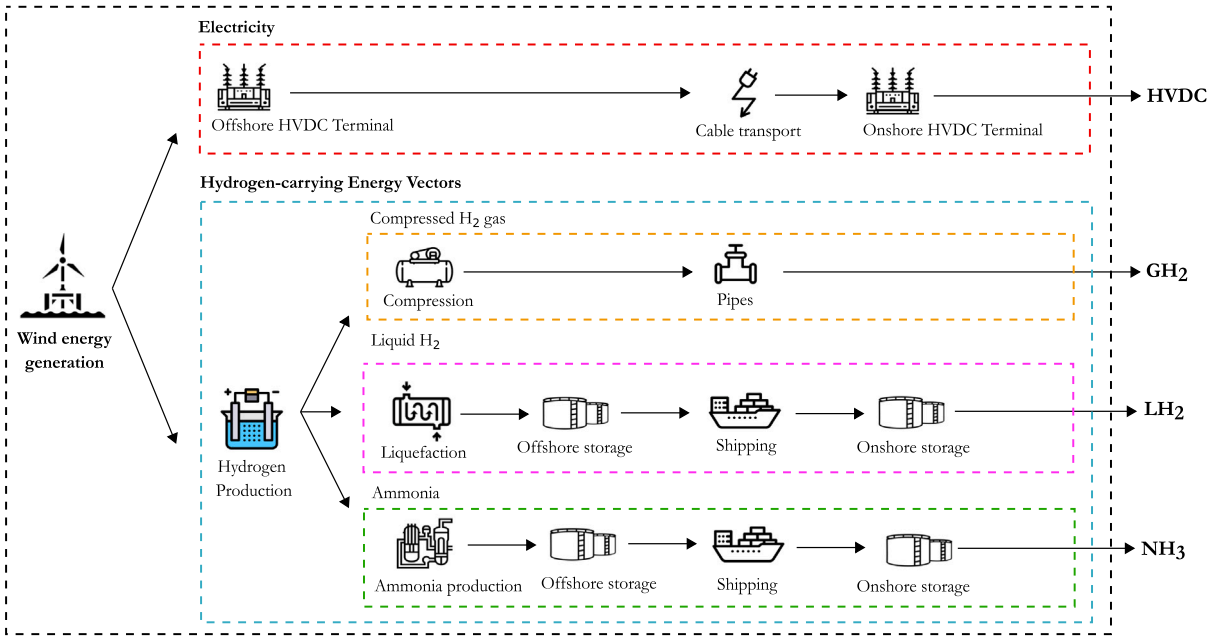

Fig. 1. Energy conversions for each energy vector.

2. Techno-economic model

In this section, the holistic model for the techno-economic assessment of far-offshore H_2-carrying energy vectors is defined. For this purpose, the energy model is described first, including the considered energy vectors, and the fundamentals and main hypotheses for energy generation, conversion, transport and storage modelling. Subsequently, the integrated-cost economic model is described, articulating the costs for all the considered elements.

2.1. Energy model

2.1.1. Definition of the energy vectors

In this study, the term energy vector refers to the form the energy takes to be delivered from the offshore wind farm to shore. Hence, the energy vectors could be electricity, transported through relatively conventional electric cables, pure H_2 in different phases, or other H_2-based fuels.

As previously mentioned in the introduction, various energy vectors have been considered for transporting the offshore-generated H_2. In this study, the vectors that require *in-situ* carbon capture have not being considered to avoid incorporating a technology that may not be feasible at the necessary scale. Vectors relying on carrier molecules have also been neglected, due to their inherent disadvantages in transporting large quantities. Consequently, the energy vectors considered within this research are (i) electricity, (ii) compressed gas hydrogen (GH_2), (iii) liquid hydrogen (LH_2) and (iv) ammonia (NH_3). As illustrated in Fig. 1, the wind energy generation model (black dashed line) is common for all the scenarios. The first full-electric scenario (red dashed line) involves the offshore and onshore electricity conversions, and the transport via submarine cables. The next three scenarios comprise the hydrogen-carrying energy vectors (blue dashed line), being the production via electrolysis common to all the vectors. Regarding the GH_2 scenario (orange dashed line), a compression stage and transport via piping is considered; while for LH_2 (pink dashed line), a liquefaction unit, onshore and offshore storage infrastructure, and transport via cargo ships are incorporated. Finally, the NH_3 scenario (green dashed line) needs an ammonia production process along with onshore and offshore storage, and transport via cargo ships.

Each energy vector considered in this study is briefly described in the following:

- **Electricity**: High voltage (HV) lines are the established choice for both existing and planned offshore wind farms, as well as the common configuration selected in the vast majority of the literature when conducting techno-economic assessment [42]. Therefore, this vector serves as a benchmark for verifying the common aspects of the model, and assessing the suitability of H_2-based energy carriers under different resource conditions and locations, both *near* and *far*-offshore. For the electricity vector, there are two types of HV lines: HVAC and HVDC. Among the two alternatives, HVDC lines are preferred for wind farms located relatively far from the connection point on shore. The break-even limit for using HVDC lines has been reported to happen at different distances, such as 60 km [42], between 120 and 250 km [43], and 87 km [44]. However, given the far-offshore assessment scope of the present model, only the HVDC alternative has been considered.
- **Compressed H_2 gas**: Hydrogen is produced in gaseous form in an electrolyser, but at a significantly lower pressure than the one required for its transportation. Therefore, a compressor is needed at the offshore installation. It can technically be transported via pipelines or ships, but the low volumetric energy density prevents shipping from being a suitable option. In fact, the International Renewable Energy Agency (IRENA) [45] reports that the capacity of current GH_2 ships would barely cover the energy cost of a 2600 km trip. Thus, pipelines are chosen as the means for transporting GH_2.
- **Liquid H_2**: Liquefied H_2 has been proposed as a potential H_2 energy vector for long distances. Due to the required cryogenic conditions, transportation via pipelines is unfeasible, meaning that special carrier ships that can ensure cryogenic conditions are required. Therefore, a liquefaction unit, intermediate offshore storage facilities and cryogenic ships are required for this vector.
- **Ammonia**: Nowadays, NH_3 is produced, traded and used in large scale, not only as an energy vector but also as an end-product, in the chemical industry. The production of fertilisers is a good example [45]. Even though it can technically be transported via pipelines, shipping is specially interesting thanks to its flexibility, allowing offshore produced NH_3 to be sold at any point in the coast according to the demand. The particularity of this vector is that an air-separation unit and a Haber–Bosch reactor

are needed for producing NH_3, in addition to the intermediate offshore storage facility and ships required for LH_2.

2.1.2. Energy generation model

Energy generation refers to the process by which wind energy is harvested with wind turbines and converted into electricity. This electricity is then transferred to a central platform or hub located in the wind farm by means of inter-array cables. As the wind resource is independent from the different energy vectors considered in the study (see Fig. 1), the wind energy production is calculated once per analysed location as a function of the wind speed of that specific location. After that, this energy production can be used as an input data to calculate the H_2 production for each carrier.

As stated in the introduction, for energy production in deep waters far from shore, FOWT and WEC devices are the most advanced technologies. However, FOWTs are significantly more mature, so only FOWT-based far-offshore energy generation is considered in this research. The production of the wind farm is first characterised for each possible wind speed values, which gives a farm power curve, analogous to a turbine power curve. To that end, the power curve of an individual turbine ($P_{turbine}$), which incorporates the effects of aerodynamic characteristics of the rotor and standard properties of the air (*e.g.* air density), is multiplied by the number of turbines in the farm ($n_{turbine}$). Then, the ideal power production is multiplied by a farm efficiency (η_{farm}), that incorporates both the aerodynamic losses due to wake effects within the farm and the electrical losses in the inter-array cables:

$$P_{farm}(u) = P_{turbine}(u) \cdot n_{turbine} \cdot \eta_{farm} \tag{1}$$

For the determination of this constant efficiency, different studies have been analysed. On the one hand, [46] studies the aerodynamic losses on a wind farm with 80 turbines on a typical layout (*i.e.* 8×10 grid with a separation of 7 rotor diameters). The losses are estimated in the range of 10 to 20% for most wind directions, while increase up to 40% for the worst directions. Assuming that a real wind farm would be optimised for the local wind climate, a 15% of constant aerodynamic loss is considered in the present study. On the other hand, [47] assesses the losses in the collection system, including inter-array cables, estimating an average loss of 2.18% for different cable types and farm layouts at rated power. Combining these two estimations, losses are assumed to be 17.18%, resulting in a farm efficiency of 0.83 ($\eta_{farm} = 0.83$).

Hence, when simulating the energy generation at one specific site and time period, the hourly wind speed data is combined with the farm power curve, providing hourly wind farm energy production estimates. The selection of the specific wind turbine and its associated power curve is described later in Section 3.

2.1.3. Energy conversion model

Energy conversion refers to the process by which the energy generated in the wind farm and transmitted to the central platform is transformed into an energy vector. This transformation is computed at different operating conditions for all the energy vectors. Therefore, a production curve is generated, which provides the production of each energy vector as a function of the power supplied from the turbines to the central hub.

In the case of electricity as an energy vector, an additional fixed loss of 5% is assumed for the transformation into direct current. This is consistent with [48], where the losses of different transmission options for offshore wind farms are estimated and validated, considering different power levels and distances. For the H_2-based vectors, the equipment can be divided into two parts: (i) the equipment required to produce H_2, which is common to all vectors and consists of an electrolyser with auxiliary equipment (*e.g.* such a desalination unit); and (ii) the equipment specific to each vector, consisting on a compressor for GH_2, a liquefier for LH_2, and an air separation unit and a Haber–Bosch reactor for NH_3. Hence, the model needs to take into account the energy consumption of the required equipment in each vector, which is also supplied by the instantaneous generation of the wind farm. In addition, the model also needs to take into account the relevant mass conversion rates. Hence, the conversion of all H_2-based energy vectors is assumed to be linear, represented by the following equation system:

$$P_{farm} = P_{elec} + P_{vector} \tag{2}$$

$$\dot{m}_{H_2} = a_{elec} \cdot P_{elec} \tag{3}$$

$$P_{vector} = b_{vector} \cdot \dot{m}_{H_2} \tag{4}$$

where, P_{farm} is the electric power available as an input of the central platform or hub, P_{elec} the electric power consumed by the electrolyser and the auxiliary elements, and P_{vector} the electric power consumed by the specific equipment required for energy vector. In addition, $\dot{m}_{H_2}$ refers to the produced H_2 mass flow rate of the electrolyser, being a_{elec} the conversion rate of the electrolyser to convert electricity into H_2, and b_{vector} the relationship between the transformed H_2 and the power consumed by the vector-specific equipment.

The procedure to solve the (2)–(4) equation system is structured as follows: For each simulated location, P_{farm} is calculated following Eq. (1). Subsequently, P_{vector} is defined as a function of P_{elec} combining Eqs. (3) and (4), where P_{elec} is obtained solving Eq. (2). Note that every location in the area of study is characterised by a different wind resource, resulting in a different energy generation. Consequently, power consumption of the electrolyser and auxiliary equipment, and the hydrogen production rate vary with the location.

For each case, the produced mass flow rate of each H_2-carrying vector ($\dot{m}_{vector}$) is calculated as follows:

$$\dot{m}_{vector} = c_{vector} \cdot \dot{m}_{H_2} \tag{5}$$

where c_{vector} is the relationship between the H_2 mass flow and the mass flow of each H_2-carrying vector. The coefficients corresponding to Eqs. (3)–(5) are shown in Table 1, including the references where these values are extracted from. It should be noted that, since the conversion coefficients are constant, dynamics and part-load efficiencies of the conversion systems (*i.e.* electrolyser, compressor, liquefier, air separation unit and Haber–Bosch reactor) are neglected, as is common in the vast majority of techno-economic models in the literature [18,32–35,49]. In fact, including models that consider those dynamics [50] in a techno-economic analysis is prohibitive in terms of computational cost, particularly when a broad spatial area is evaluated.

It should be noted that the parameter a_{elec} defined in Table 1 does not include seawater desalination. However, [51] concludes that the desalination process only represents about 1% of the total energy consumption, meaning that the energy consumption of the desalination process can be neglected.

Table 1
Coefficients of the different H_2-based energy vectors.

Coefficient	Value	Units	Reference
a_{elec}	0.0197	t/MWh	[49]
b_{GH_2}	0.98	MWh/t	[18]
b_{LH_2}	6.40	MWh/t	[18]
b_{NH_3}	3.62	MWh/t	[18]
c_{GH_2}	1	t/t	–
c_{LH_2}	1	t/t	–
c_{NH_3}	5.56	t/t	[49]

2.1.4. Energy transport and storage model

After the conversion stage, all energy vectors need to be transported to shore. In this study, a single discharge port is assigned to each location across the analysed area, so that a single transport cost is computed for each energy vector and location. For HVDC and GH_2, transport to shore is assumed to be instantaneous, while losses and

Table 2
Parameters for the shipping simulations [19].

Parameter	Value	Units
LH_2 ship capacity	11 000	t of LH_2
NH_3 ship capacity	53 000	t of NH_3
Ship loading time	2	days
Ship unloading time	2	days
Ship speed	32	km/h

energy needs are considered in the conversion model described in the previous section.

In contrast, since LH_2 and NH_3 require shipping, two intermediate storage facilities need to be incorporated into the model: the offshore storage holds the produced energy vector until a ship is available, while the onshore storage receives and holds the shipment to ensure a constant supply to the end-user at the harbour. For each geographical location and energy vector, a time domain simulation tracks the levels of both storage facilities and the availability of ships for the whole lifetime of the project. The shipping simulation takes a series of parameters as inputs, as shown in Table 2. These values are taken from [19], except for the unloading time, which is assumed to be the same as the loading time.

To calculate the optimal number of ships and size of the storage, the mass flow rate of the produced LH_2 and NH_3 is used following Eq. (5). Considering both production rates along with the ship capacities, speed and loading times defined in Table 2, an iterative process determines the optimum number of ships in order to maximise their time of use. Finally, the dimensions of each storage is defined based on the difference between the minimum and the maximum offshore and onshore volumes achieved during the whole lifetime, ensuring that all the produced H_2, regardless of the energy vector, is transported to the harbour. Further optimisations regarding the optimal size of the vessels are considered out of the scope of this work.

To sum up, the shipping simulation provides the following information for each location and energy vector: (i) the optimal number of vessels serving that farm, (ii) the amount of time, over the whole lifetime, that each vessel is actively used, (iii) the time series of the storage levels over the whole lifetime, and, as a consequence, (iii) the offshore and onshore storage capacity.

2.2. Integrated cost model

2.2.1. General structure

The integrated cost is estimated for each location and energy vector. The final cost is divided into different concepts, some of them being common to all energy vectors, while others are specific to each vector. Hence, each concept is composed of three expenditures: capital expenditure (CAPEX), operational expenditure (OPEX) and decommissioning expenditure (DECEX). The euro has been used as the default currency and a conversion rate of 1.19 €/$, computed as the mean conversion rate between 2003 and 2023 [52], has been used to convert the costs provided in $ in the literature. These three expenditures are then converted into the Total Cost of Ownership (TCO) discounted to the year 0 of the project following the expression:

$$TCO = TCO_{CAPEX} + TCO_{OPEX} + TCO_{DECEX} \tag{6}$$

where TCO_{CAPEX}, TCO_{OPEX} and TCO_{DECEX} are the contributions of each expenditure to the TCO.

Hence, the expenditures are distributed over time, with the CAPEX being spent in the first year, the OPEX being uniformly distributed throughout the whole project's lifetime and the DECEX being allocated for the final year. To consolidate the expenditures at year 0, the contributions are calculated as follows:

$$TCO_{CAPEX} = CAPEX \tag{7}$$

$$TCO_{OPEX} = \sum_{i=1}^{N} \frac{OPEX/N}{(1+r)^i} \tag{8}$$

$$TCO_{DECEX} = \frac{DECEX}{(1+r)^N} \tag{9}$$

where N is the lifetime of the project in years and r the discount rate, for which a value of 8% is used, since it is the weighted average cost of capital commonly used for offshore wind projects in developed countries [53]. The discount rate is one of the variables with the largest impact on the final cost of energy [54] and, thus, a sensitivity analysis of the TCO to different r values is an interesting analysis. However, this analysis is beyond the scope of this work.

The specific costs for the different elements have been calculated using different values and functions found in the literature. A detailed breakdown of the cost calculation process is given in the following subsections.

2.2.2. CAPEX

CAPEX refers to the funds a company uses to acquire and maintain its fixed assets such as properties, plants, buildings, technology or equipment. Considered CAPEX values for energy generation, conversion, transport and storage of far-offshore H_2-based vector projects are described here.

Energy generation. The CAPEX related to the energy generation considers costs for (i) developing and consent, and (ii) the wind farm, including turbines, mooring systems, foundations and inter-array cables. All the costs related to the energy generation stage are common to all energy vectors.

As defined in [15], developing and consenting costs include environmental, seabed and met station surveys along with project management and development services. Although these costs can reach up to 4% of the total CAPEX, [15] suggests to incorporate the UK government data, establishing a cost of 210 k€/MW [55]. Although [15] only includes the costs for projects equivalent to the HVDC connection, the present study assumes that every energy vector would have the same developing and consenting costs.

For the turbine and platform, the manufacture of the turbine is assumed to cost 1.6 M€per MW [15,56], while the cost of manufacturing the platform is considered 8 M€ [15,56]. The CAPEX for the installation costs of these two components depends on the distance to the port and is given as follows [15,57]:

$$C_{inst,turb} = n_{turb} \cdot (T_{inst} + 2 \cdot d/V_{tug}) \cdot C_{tug}/n_{turb,trip} \tag{10}$$

where n_{turb} is the number of turbines, T_{inst} the amount of days to install each turbine and foundation (assumed to be 2), d the distance to the closest port from each location given in kilometres, V_{tug} the speed of the tugboat (assumed to be 480 km/day), C_{tug} the cost of renting the tugboat, and $n_{turb,trip}$ the amount of turbines that can be carried per trip (assumed to be 5).

For the manufacture of the moorings, the following expression and assumptions are considered [15]:

$$C_{moor} = n_{turb} \cdot n_{lin} \cdot (C_{anch} + (1.5h + 410) \cdot C_{lin} + 50 \cdot C_{ch}) \tag{11}$$

where n_{lin} is the number of mooring lines per turbine/floater (assumed to be 4 in this case), C_{anch} the cost of an individual anchor, h the water depth of the site, in metres, and C_{lin} and C_{ch} are, respectively, the cost of each mooring line and chain section per unit of length. Each mooring line is assumed to be a combination of steel, wire and chains, the part in contact with the seabed being necessarily a chain section. The installation of the moorings costs are estimated in about 240 k€per turbine [15,56].

The manufacture of the inter-array cables is assumed to be 303.5 k€/km [15], while the installation is given as function of the distance to port: 212.3 k€/km. Although the cost model of the energy generation

Table 3
CAPEX unitary costs for energy generation.

Item	Unitary cost	Ref.
Development and consenting	210 k€/MW	[55]
Turbine manufacture	1.6 M€/MW	[15,56]
Floater manufacture	8 M€/turbine	[15,56]
Turbine and floater installation	Eq. (10)	[15,57]
Mooring manufacture	Eq. (11)	[15]
Mooring installation	240 k€/turbine	[15,56]
Inter-array cables manufacture	303.5 k€/km	[15]
Inter-array cables installation	212.3 k€/km	[15]
Central hub	62.15 k€/MW	[18]
C_{tug}	19.5 k€/day	[15,57]
C_{anch}	123 k€	[15,56]
C_{lin}	48 €/m	[15,28]
C_{ch}	270 €/m	[15,28]

Table 4
CAPEX unitary costs for energy conversion.

Item	Unitary cost	Ref.
Offshore HVDC substation manufacture	285.4 M€	[15,57]
Offshore HVDC substation installation	20 M€/substation	[15,28]
Electrolysis plant	700 k$/MW	[58]
GH_2 compressor	16 k€/tH_2/day	[18]
LH_2 liquefaction unit	2 M€/tH_2/day	[18]
Air separation and Haber–Bosch reactor for NH_3	990 k€/tH_2/day	[18]

stage is almost completely reproduced from [15], an addition cost related to the central hub is also considered. Concretely, the CAPEX for the central hub is 62.15 k€per installed MW [18], where the specific equipment required by each energy vector is neglected. The summary of the unitary costs for all aforementioned elements is shown in Table 3.

Energy conversion. The CAPEX of the energy conversion stage varies significantly depending on the energy vector, since different processes are necessary in each conversion. In the case of the full-electric HVDC alternative, the CAPEX of the offshore substation is divided between the manufacture, which is estimated in 285.4 M€ [15,57], and the installation, being 20 M€per substation [15,28].

The rest of the H_2-based vectors require an electrolyser, although its nominal power is set independently for each possible wind farm power and energy vector. This nominal power is determined by solving the equation system explained in Section 2.1.3 based upon the nominal power of the wind farm. The cost for the electrolyser and its auxiliary equipment is considered to be 700 k$ per MW [58]. In addition, the costs of the vector-specific equipment need to be considered which include a compressor for GH_2, a liquefaction unit for LH_2, and an Air Separation Unit and a Haber–Bosch reactor for NH_3. The costs for each equipment are calculated following [18] and the summary of the unitary costs for all aforementioned elements is shown in Table 4. Note that, in this study, the sizing of the equipment varies with the mean daily production. Therefore, the associated costs are also dependent on the specific location and studied time period.

Energy transport and storage. The transport and storage CAPEX also varies with each energy vector. The transport of energy in the case of HVDC includes export cables and an onshore substation. In this regard, [15] assumes that 3 export cables are needed, for which a cost of 1.168 M€per km is considered for the manufacture [57] and 637 k€per km for the installation [15]. On the other hand, the cost of the onshore substation is assumed to be constant, *i.e.* 84.35 M€, which includes both manufacture and installation costs [15].

Regarding the transport and storage of H_2-based vectors, the costs of the GH_2 considers the onshore terminal and pipelines, assuming an internal pipe diameter of 20 cm. Note that no storage is needed in the case of GH_2. In contrast, the cost of storage per tonne of fuel, both for LH_2 and NH_3, are provided in Table 5, following the costs presented in [18].

Table 5
CAPEX unitary costs for energy transport and storage.

Item	Unitary cost	Ref.
Export HVDC cable manufacture	1.168 M€/km	[15,57]
Export HVDC cable installation	637 k€/km	[15]
Onshore HVDC substation manufacture and installation	84.35 M€	[15]
GH_2 pipe	563.4 k€/km	[18]
LH_2 storage	81.13 k€/tH_2	[18]
NH_3 storage	7.99 k€/tH_2	[18]
LH_2 vessel	412 M€	[19]
NH_3 vessel	85 M€	[19]

Finally, the shipping costs are computed based upon the simulations for each site and energy vector. The cost of the vessels for LH_2 is estimated in 412 M€ [19] based on the characteristics previously described in Table 2, while the vessels for NH_3 are estimated to cost 85 M€ [19]. It should be noted that the capacity of the available vessels exceeds considerably the needs of the case study considered in the present paper, meaning that a single vessel satisfies all the transportation needs for each and every location. The summary of the unitary costs for all aforementioned elements is shown in Table 5.

2.2.3. OPEX

The operation and maintenance (O&M) costs include repairs of different components and equipment, along with the O&M fleet and crew. For the energy conversion stage, the OPEX is established as a fixed percentage of the CAPEX, although the percentage varies for each auxiliary equipment: 1.5% for the electrolyser and its auxiliary equipment (thermal management unit, desalination plant, product gases conditioning) [58], 4% for the compressor in GH_2 [18], 4% for the liquefaction unit in LH_2 [18] and 2% for the air separation unit and the Haber–Bosch reactor in NH_3 [18]. With respect to the energy transport stage, the OPEX of the vessels is defined as 5550 €per day for both LH_2 and NH_3 [19]. Hence, the final OPEX for the shipping is computed based on the accumulated usage time of the vessels. Regarding the energy generation stage, no reliable reference that includes comprehensive O&M costs for H_2 production is found in the literature. Therefore, the OPEX for the generation stage is determined as the 4.5% of the CAPEX in the present study, assuming a conservative approach that is consistent with the conversion and transportation stages.

2.2.4. DECEX

Finally, the DECEX includes the cost of all administrative and technical activities of the decommissioning stage, aiming to eliminate or minimise the residual hazards in the facility. However, since no real-life offshore wind project has reached this stage, the uncertainty about its cost is remarkable [15]. In this regard, the DECEX for each component is given as a percentage of its installation costs, as defined in [15]: 70% for the turbines and floaters, 90% for the moorings, 10% for the inter-array cables and 10% for the HVDC substation.

2.2.5. Levelised costs

The total amount of energy vector delivered into the harbour and the costs associated to each energy vector over the lifetime are combined to compute the LCOE and the Levelised Cost of Energy Vector (LCOEV) for each location across the area of study. The LCOE expresses the cost of each unit of energy for a given project, but it can also be understood as the price at which the energy should be sold so that the Net Present Value of a project becomes 0. In the scope of the present study, the LCOE allows the comparison of the different sites and energy vectors, as the unit is the same for all vectors (€/MJ).

The LCOEV is provides the same information as the LCOE, except that the LCOEV expresses the cost of each energy vector via the vector-specific unit, *i.e.* €/MWh for HVDC or €/t for H_2-carrying vectors.

Therefore, the LCOEV does not allow a direct comparison among the different vectors. However, it is a convenient metric for comparing the results of the present study against market prices and/or other studies in the literature. The total production of each energy vector over the whole lifetime is assumed to be sold at a constant rate along the lifetime of the project, assuming a constant Annual Energy Vector Production (AEVP). Therefore, the expression for the LCOEV is calculated as follows:

$$LCOEV = \frac{TCO}{\sum_{i=1}^{N} AEVP/(1+r)^i} \quad (12)$$

In the case of the full-electric HVDC alternative, a simple unit conversion between MWh and MJ is considered in order to enable the comparison with other H_2-carrying vectors, while the Lower Heating Values (LHV) for H_2 and NH_3 are used for the H_2-based vectors: a LHV of 120 MJ/kg for GH_2 and LH_2, and 18.9 MJ/kg for NH_3.

3. Case study

The following section defines the case study to which the techno-economic model described in Section 2 is applied. To that end, the FOWT technology used for far-offshore energy generation is first selected and described. Then, the studied geographical area is specified along with the information about the location of the main ports, the distance between each location and the closest port, and the bathymetry. Finally, the wind data used in the offshore energy generation model is defined.

3.1. FOWT technology and farm design

The same wind turbine and farm size are assumed for all sites. In the case of the turbine, since FOWTs are supposed to operate with very large turbines (over 10 MW), the power curve of the IEA 10 MW reference turbine is used [59]. Its power curve is presented in Fig. 2. All turbines at all sites are assumed to use a semi-submersible floater as a platform, since it is the most versatile and, overall, most appropriate wind turbine platform for this area [60]. An example of such a FOWT is shown in Fig. 3. Hence, the farm is assumed to be composed of 100 turbines, resulting in 1 GW of rated power.

3.2. Geographical area

This study considers the area off the Iberian Peninsula for the techno-economic assessment. The selection of this area is justified by its vast renewable energy resource and the remarkable role of the Iberian Peninsula in the decarbonisation of the European Union through green H_2 [10]. Hence, the most important harbours along the coast of the Iberian Peninsula and the Balearic Islands are selected, assuming that each grid-point in the analysed geographical area uses the closest harbour for installation, operation, energy delivery and decommissioning. All considered harbours are geographically represented in Fig. 4 and listed in Appendix A based upon the information provided in [62].

Fig. 3. Example of a semi-submersible platform [61].

Additionally, the bathymetry, and the distance between each location and the closest port are illustrated, respectively, in Fig. 5(a) and (b). Although several studies have set the limit for technical feasibility of FOWT farms at 1000 m [63–65], the bathymetry map suggests that the surroundings of the Iberian Peninsula and Balearic Islands tend to become very deep (beyond the 1000-metre limit) relatively close to the shore. However, the techno-economic tool presented here is also aimed to assess very far-offshore locations where the water depth will commonly exceed the 1000-metre limit. Hence, the water-depth limitation is ignored in this study and the whole area or study is considered regardless of the water depth.

3.3. Wind data

In Fig. 6(a) and (b), the average wind speed and the Capacity Factor (CF) associated to the selected FOWT technology are illustrated, respectively, across the whole area of study. The wind speed and, as a consequence, the CF are computed using ERA5 reanalysis data [66] for

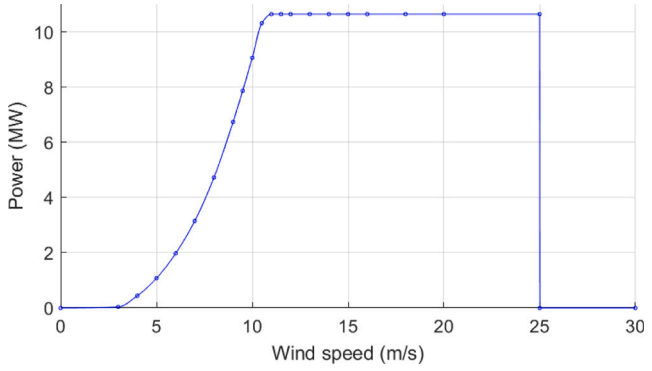

Fig. 2. Power curve for the reference 10MW turbine from the IEA.

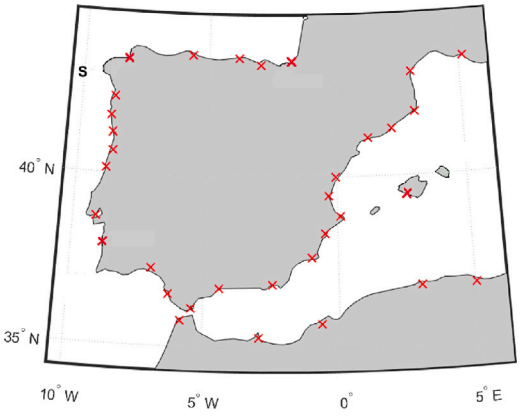

Fig. 4. Selected sites and harbours.

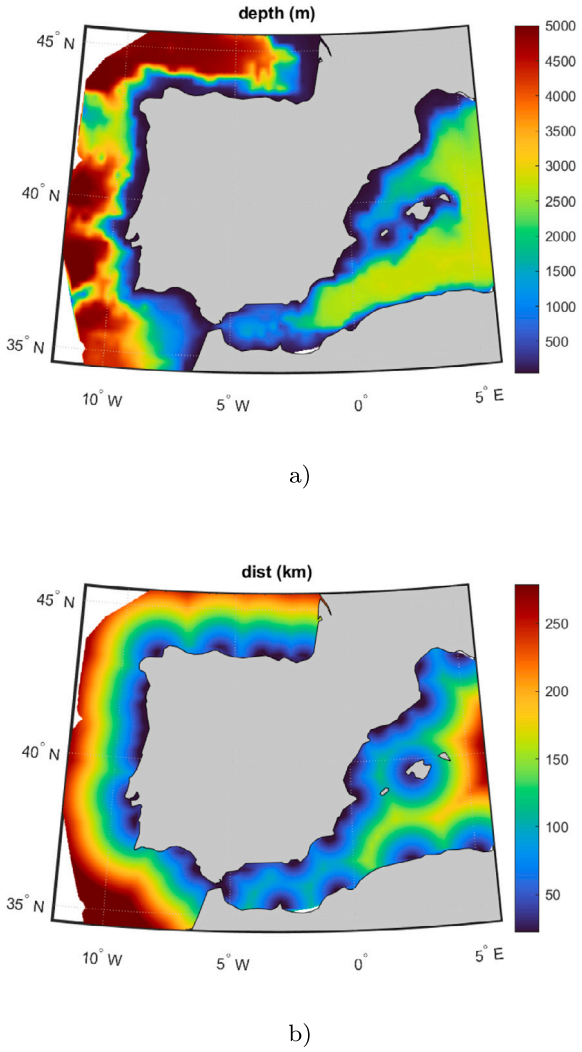

Fig. 5. Geographical data of the analysed area: (a) Bathymetry, and (b) Distance to port.

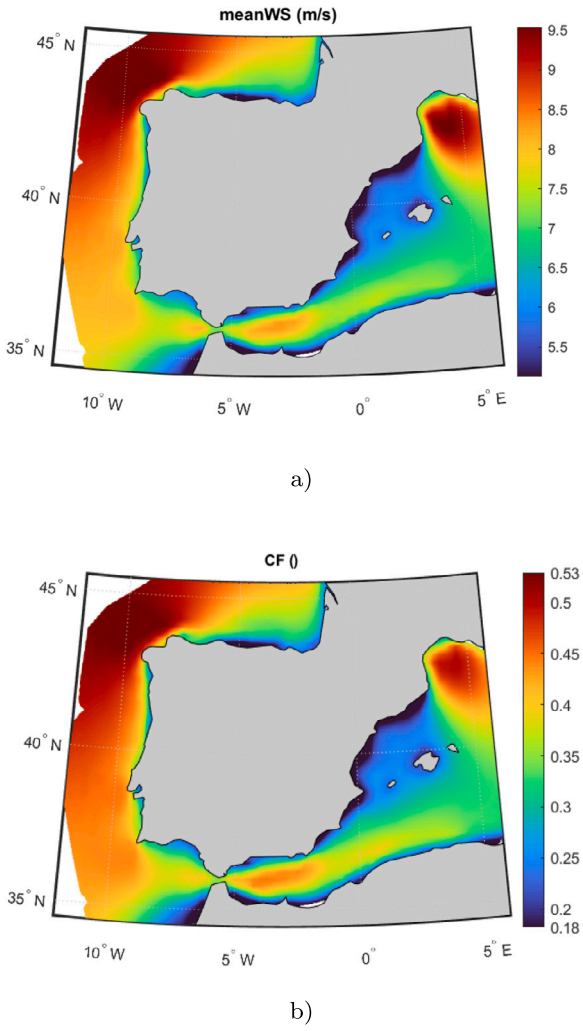

Fig. 6. Wind data in the analysed area: (a) Mean Wind Speed, and (b) Capacity Factor (CF).

the period between 1990 and 2019, resulting in a lifetime of 30 years. In fact, the simulated locations correspond to ERA5 gridpoints avoiding the interpolation of the data. With a spatial resolution of 0.25°, a total number of 1493 gridpoints are considered in the selected area. Note that the production of the wind farm is calculated using the wind speed module at 100 m height, which is the reference height provided by ERA5 that is closest to the turbine hub.

3.4. Summary of the methodology

As a summary of the different aspects of the case study, the implementation of the techno-economic tool on the present case study is briefly described:

- First, wind speed data from the ERA5 reanalysis are considered along with basic information for each potential location, such as water depth and distance to the closest major port.
- Subsequently, the time series for power generation is computed for the selected wind farm configuration based on the turbine power curve and the farm efficiency.
- Afterwards, the conversion of electricity into the four selected energy vectors is simulated using conversion factors, efficiencies, mass ratios, and energy consumption data specific to each energy vector. Afterwards, the transport of each energy vector to the harbour is analysed, which provides the total amount of delivered energy, dimensions of the storage facilities and the number of vessels employed for the transport.
- Finally, the costs associated with each energy vector and wind farm location are calculated, and the techno-economic assessment is mapped across the entire study area for each energy vector.

4. Results and discussion

In the following section, simulation results are presented and discussed. To that end, the outcomes of the present study are first compared with different results provided in the literature in order to verify the reliability of the techno-economic model. Subsequently, the LCOEV, LCOE, and TCO are mapped across the entire study area. The results are complemented with a sensitivity analysis to assess the influence of the CF, the distance to the port, and water depth on the final cost of the different energy vectors.

4.1. Model verification

For the model verification, the LCOEV values obtained in this study are compared with bibliography and shown in Table 6. To that end, different statistical values based on all the results computed across the

Table 6
Levelised Costs of Energy Vectors: Verifying against literature results.

	HVDC (€/MWh)	GH_2 (€/kg)	LH_2 (€/kg)	NH_3 (€/kg)
Min	83.35	4.20	10.96	1.55
Avg	132.83	6.68	17.29	2.32
Max	1045.01	52.57	110.88	14.21
P05	90.21	4.53	11.65	1.62
Q1	103.12	5.19	14.03	1.91
Q2	119.74	6.02	15.79	2.12
Q3	144.81	7.27	19.07	2.53
P95	215.14	10.84	27.01	3.53
[15]	95–160	–	–	–
[63]	150–1000	–	–	–
[67]	100–250	–	–	–
[18]	–	5.2–7.5	6.5–7.8	1.3-1.53
[34]	–	2.5–9.0	2.0–15.0	–
[33]	–	2.0–5.6	–	–

whole geographical area are considered: minimum (Min), maximum (Max) and averages values (Avg); the 5th (P05) and 95th (P95) percentiles; and 1st (Q1), 2nd (Q2) and 3rd (Q3) quartiles. The LCOEV is influenced by all the steps of the model and, thus, it can be considered as a good indicator of the model reliability.

Table 6 shows that the averaged results for HVDC fall within the expected range. Since the reference studies presented in the literature include the effect of the temporal and spatial variability of the wind resource, results can be directly compared. Additionally, the extensive available literature, including historical data from real wind farms [67], reinforces confidence in the results obtained with the techno-economic tool presented here. Finally, as the largest part of the cost for HVDC projects corresponds to the aspects that are common to all energy vectors, the agreement of the HVDC results with the literature provides a reliable basis for other vectors.

Regarding the H_2-carrying energy vectors (*i.e.* GH_2, LH_2, NH_3), the comparison with the literature is not as direct as in the case of HVDC. For example, it should be noted that [18,34] do not consider the variability of the wind resource in their calculations. Indeed, they assume relative high CFs (around 0.5) that represent locations of a significantly high wind resource. As a consequence, since realistic wind resource data results in lower CFs in the majority of locations, it is expected that the average LCOEV values from the present study result higher than LCOEV values of the literature. In fact, the area studied in the present paper shows maximum CFs slightly above 0.5 (see Fig. 6). Therefore, for model validation purposes, the P05 value is considered adequate, even conservative, as it falls below the capacity factors assumed in the literature. Hence, P05 LCOEV values for GH_2 and LH_2 express a good agreement, lying in the range observed in the literature. In the case of NH_3, the agreement is also relatively good, exceeding the upper bound of the range by only 4%. In conclusion, considering the uncertainties involved in the comparison, the techno-economic tool developed within this work is considered validated for all energy considered energy vectors.

4.2. Levelised Cost of Energy Vectors (LCOEV)

Fig. 7 illustrates the levelised cost for each energy vector mapped for the whole area of study. To prevent outliers from obstructing

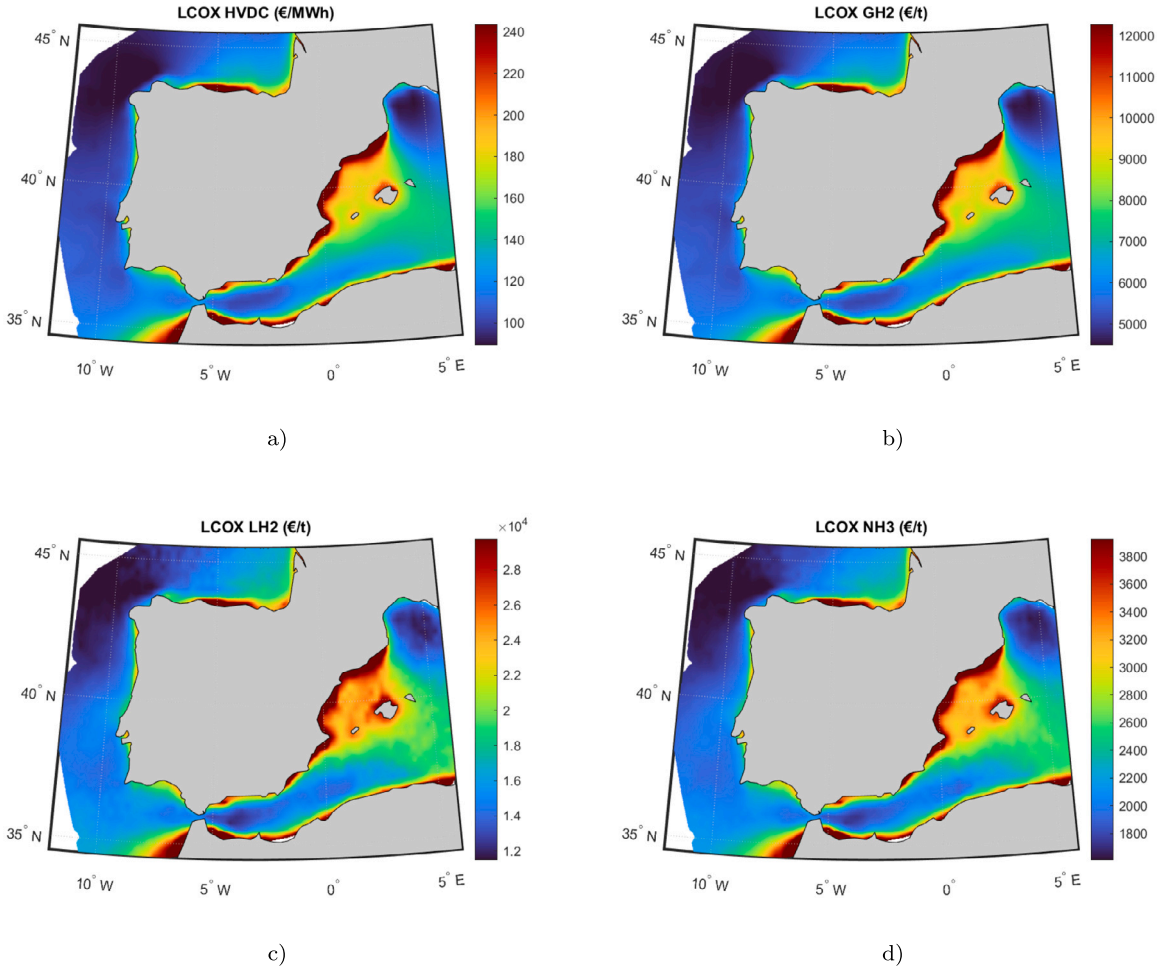

Fig. 7. Levelised Cost of Energy Vectors: (a) HVDC, (b) GH_2, (c) LH_2 and (d) NH_3.

the visualisation, the range for all of the maps shown here has been adjusted to cover the results between the 5th to the 95th percentile. The values that exceed those limits are simply shown in the colours corresponding to the bounds of the range.

The comparison between Figs. 6 and 7 shows that the areas with the highest LCOEV values match with the lowest wind speed and CFs areas, which correspond to the nearshore coastal areas. This confirms that the wind resource is a crucial factor for site-selection. Hence, the most appealing areas are shown to be identical for all energy vectors: The Galician coast in the North-West of Spain, the Alboran Sean in the South of Spain and the Gulf of Lion in the South-East coast of France. Interestingly, both the bathymetry and the distance to shore/harbour are shown to have a reduced influence on the final LCOEV regardless of the energy vector.

4.3. Levelised cost of energy (LCOE)

The LCOEs are proportional to the LCOEVs, as explained in Section 2.2, but they are expressed in the same units (€/MJ) for all energy vectors, allowing for comparison between them. Fig. 8 shows the LCOE maps with the same colour code for all the energy vectors, making comparison straightforward. In these mapped figures the following can be observed:

- For any given site, HVDC is always the cheapest energy vector, followed closely by GH_2. A significant difference exists for the other two energy vectors, LH_2 always being the most expensive alternative.
- Even when comparing vectors across different sites, for reasonable CF values (>0.25), the shipped energy vectors (*i.e.* LH_2 and NH_3) are always more expensive than the non-shipped ones (*i.e.* HVDC and GH_2). In fact, even the site with the lowest LCOE for NH_3 is costlier than the most expensive site with GH_2.

To gain further insights, Fig. 9(a) and (b) show, respectively, LCOE values for the whole are of study plotted against the CF and the distance to port. In both of these scatter plots, the points on the same vertical line correspond to the same site, as the CF and the distance do not change with the energy vector. From these results, the following can be concluded:

- The wind speed and, as a consequence, the CF are very good predictors of the levelised cost for any given energy vector.
- The distance to port is not a good predictor of the levelised cost. The increase in wind resource (higher CF) when moving further away from shore is shown to have a compensating effect, which cancels out the extra cost associated with the longer distance.

Based on this specific case study, it can be stated that H_2-based energy vectors, regardless of its form, are not able to compete with the full-electric HVDC alternative, at least when the only considered factor is the economic cost of bringing energy to shore. This stands for all locations, even the ones further from shore, where H_2-based vectors were expected to have an economic advantage. However, not all H_2-based vectors are equal in this regard: while the costs for GH_2

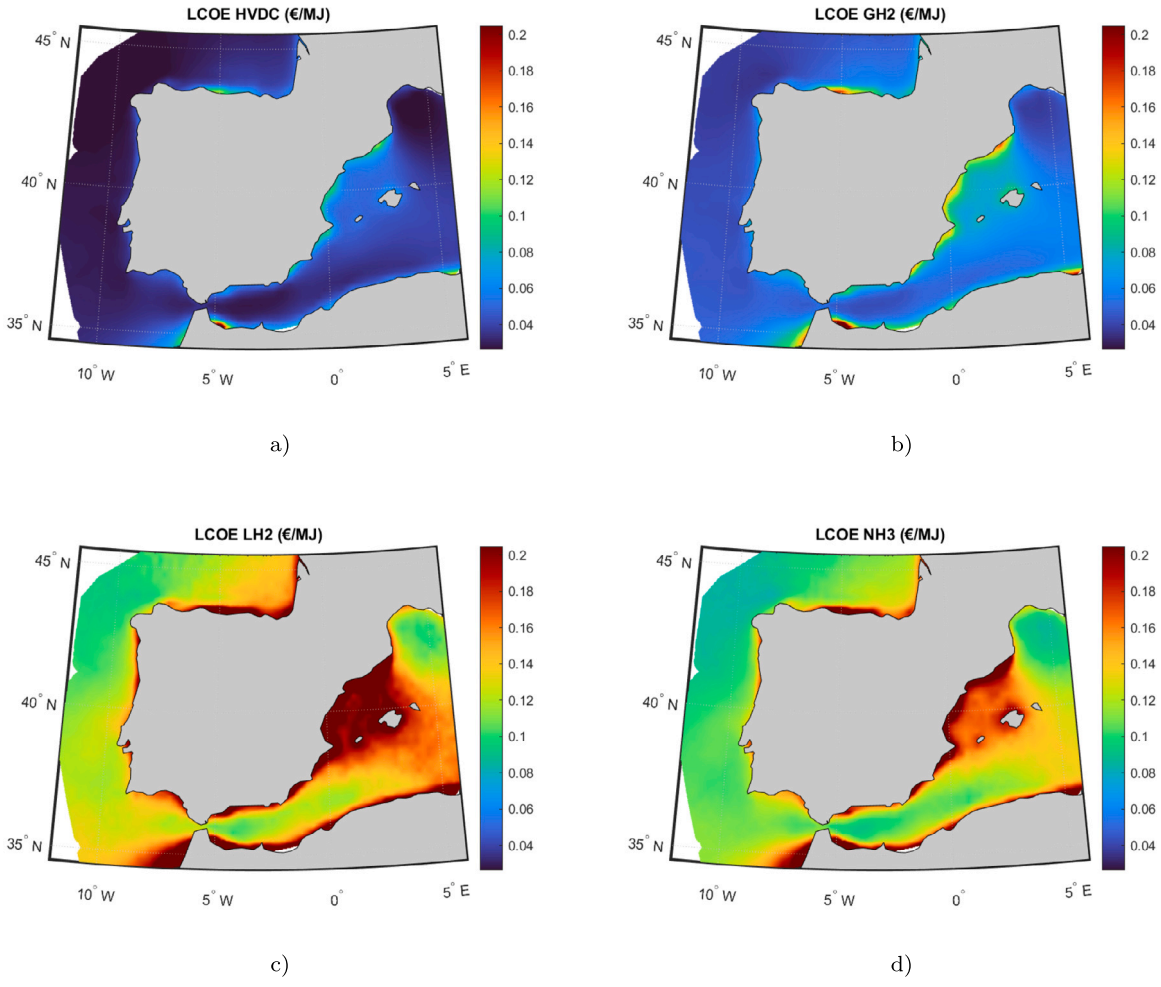

Fig. 8. Levelised Cost of Energy: (a) HVDC, (b) GH_2, (c) LH_2 and (d) NH_3.

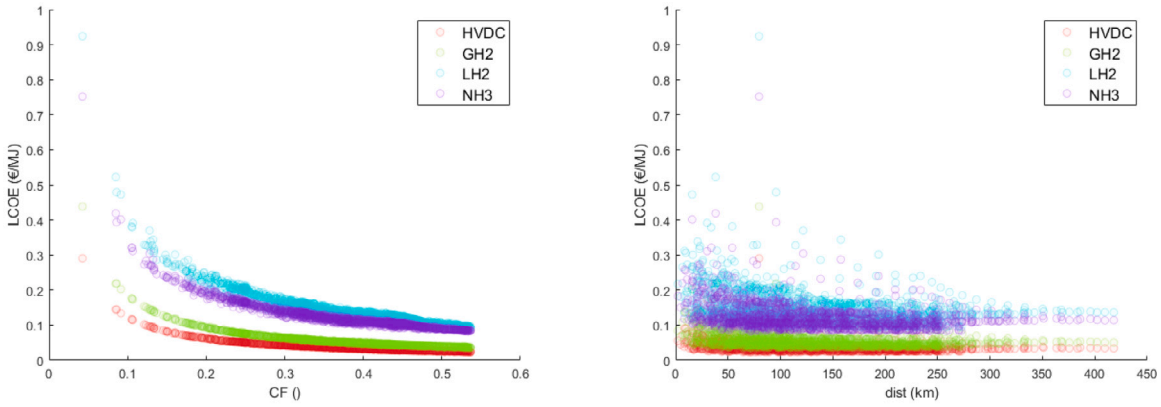

Fig. 9. LCOE sensitivity analysis: (a) Effect of Capacity Factor (CF), (b) Effect of distance to port. HVDC depicted in red, GH_2 in green, LH_2 in blue, and NH_3 in purple.

are similar to HVDC, the costs of shipped energy vectors (*i.e.* NH_3 and LH_2) are an order of magnitude higher.

4.4. Total Cost of Ownership (TCO)

Finally, total expenses are analysed by means of the TCO, which provide the most interesting results for decision makers and investors. The TCO incorporates all the expenses over the project lifetime discounted to the beginning of the project.

Fig. 10 illustrates the TCO for each energy vector mapped over the whole area of study, using the same colour legend for all vectors. The hierarchy between vectors remains as for the LCOE: HVDC is always the cheapest option followed closely by GH_2, with NH_3 and LH_2 falling well behind, being LH_2 the most expensive option. Similarly to other

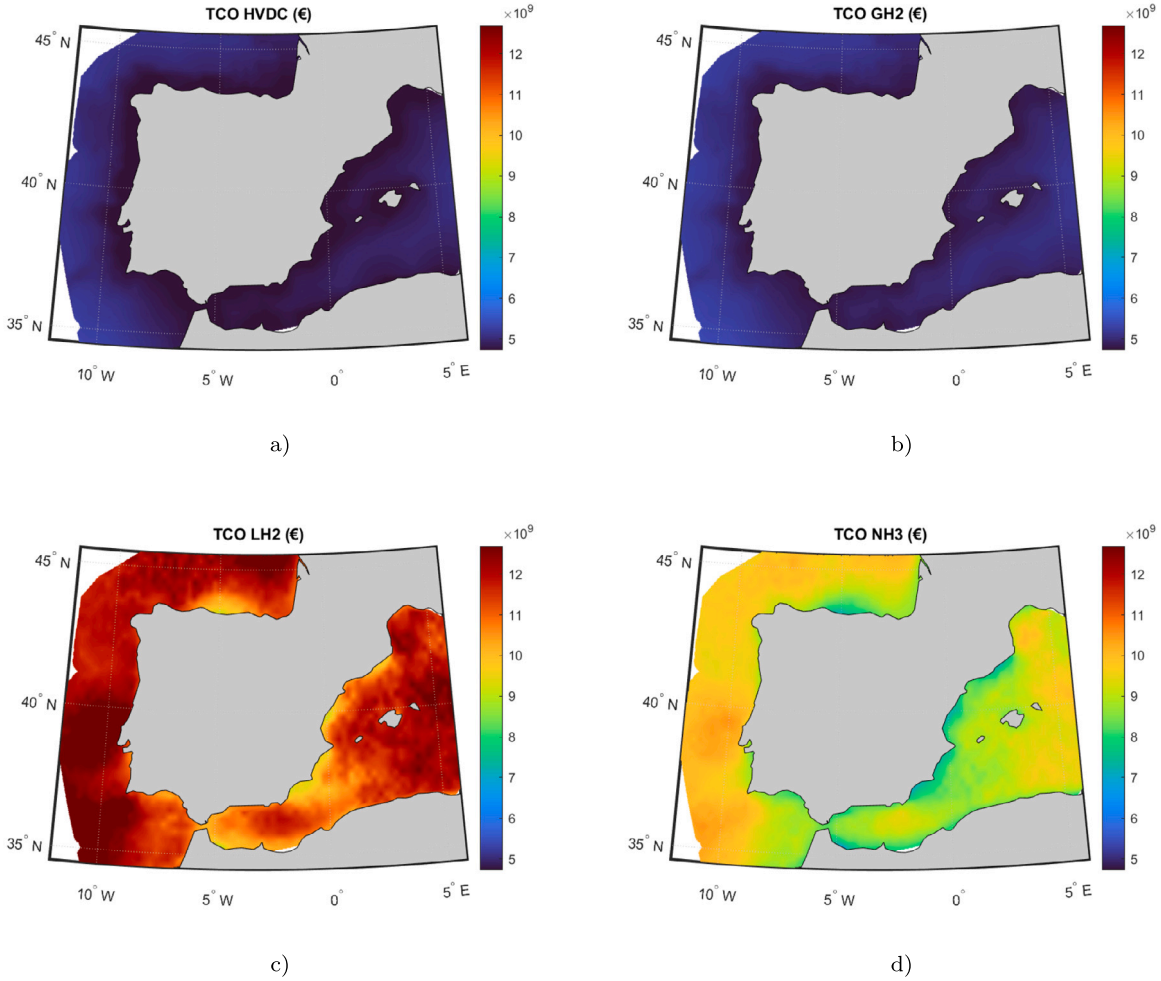

Fig. 10. Total Cost of Ownership: (a) HVDC, (b) GH_2, (c) LH_2 and (d) NH_3.

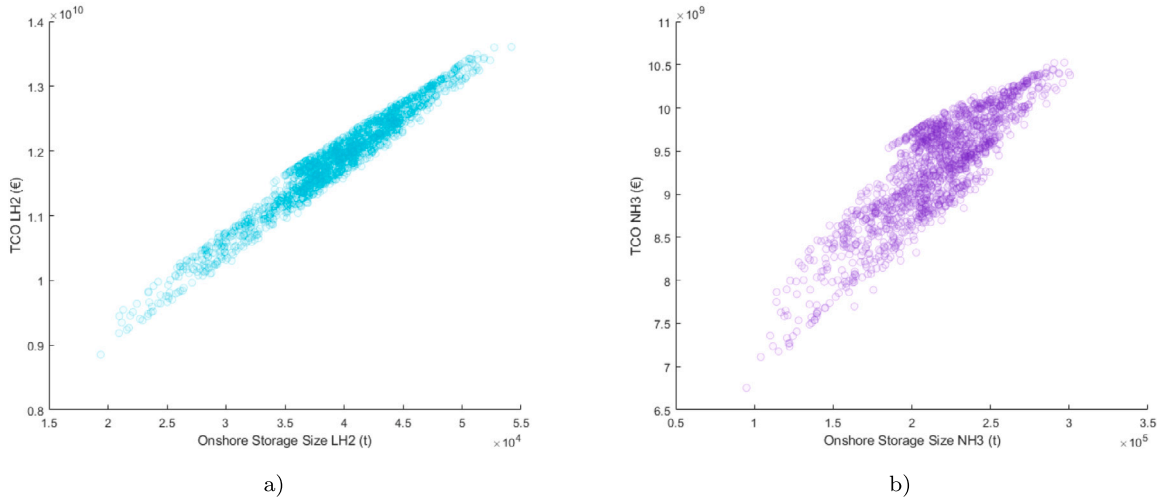

Fig. 11. Effect of onshore storage size in the TCO for (a) LH_2 and (b) NH_3.

metrics, the shipped energy vectors (*i.e.* LH_2 and NH_3) results around two- to three- times more expensive than the other two (*i.e.* HVDC and GH_2).

With respect to the sensitivity to different variables, Figs. B.1 to B.3 depicted in Appendix B show that the influence of the bathymetry and the distance to port on the TCO is lower for the shipped vectors due to their higher total expenses. Similarly, Fig. B.3 illustrates the impact of CF, showing that the CF is the most dominant variable for TCO. However, no clear trend is identified for the impact of the CF on the HVDC and GH_2 vectors, showing a significantly larger dispersion. The main reason for this is that, in the model, the cost of energy conversion and transport means for the HVDC option does not depend on energy generation, since the cost of electrical cables and pipelines depend only on the distance. Similarly, in the case of the GH_2 vector, the cost of the compressor does depend on the mean daily production, but it is negligible compared to other costs. On the other hand, the expenses for the shipped energy vectors are proportional to the CF. This happens because the costs of the offshore storage and shipping increase with the energy generation.

Nevertheless, the most important factor for the TCO of the shipped energy vectors is the onshore storage capacity, as shown in Fig. 11. The expenses for the whole project are shown to be linearly proportional to the dimensions of the onshore storage facility, with LH_2 showing a steeper slope than NH_3. This issue with the onshore storage capacity suggests that the assumptions considered for sizing the storage facility may have been too restrictive.

As explained in Section 2.1.4, the shipped energy vectors deliver the H_2-carrier to the onshore storage at a constant rate along the whole lifetime. This would be akin to a client buying the vector at a constant rate at the harbour. However, these assumptions seem to generate oversized onshore storage facilities, creating a biased comparison framework where only the shipped H_2-based energy vectors consider the cost of an onshore facility to manage the integration of the energy into the national grid. In fact, both the all-electric HVDC and the GH_2 vectors have important and expensive infrastructure where the fluctuations of the supply are managed. However, the cost of such a infrastructure in not involved in the cost of the energy vector.

Hence, in order to be fair with the shipped H_2-based energy vectors, a new unbiased comparison framework is suggested, where the cost of the onshore storage infrastructure is neglected for all energy vectors. Hence, it is assumed that both LH_2 and NH_3 are integrated into the market the moment they arrive to the harbour, similarly to the HVDC and GH_2 vectors. Nevertheless, it must be noted that onshore storage is crucial for an adequate management of LH_2 and NH_3 vectors, so that all the production can be absorbed by the demand. This does not pose such a problem in the case of HVDC and GH_2 because the inertia of the already existing infrastructures, *i.e.* the electrical grid and the gas distribution pipelines, respectively, can handle the imbalance between the production and the demand. However, the main question is whether the producer should take responsibility to pay for and manage such imbalance or it should be an external (public) body, as in the case of HVDC and GH_2. Given the immaturity of the technologies and the fact that the uncertainty remains, both frameworks are studied in the present study.

4.5. Techno-economic analysis without onshore storage

Fig. 12(a) and (b) respectively show the effect of the CF in LCOE and TCO when the cost of the onshore storage infrastructure is ignored. In this case, the following can be concluded:

- 12(a) shows that LH_2 and NH_3 remain as the costlier vectors for every simulated location. However, in the locations where the CF is higher, LH_2 and NH_3 appear to be more competitive, significantly reducing the differences with the more conventional GH_2 and HVDC.
- The slopes of the TCO trends shown in 12(b) for LH_2 and NH_3 suggest that, as the CF increases, LH_2 becomes more appealing. Although LH_2 storage and conversion costs are higher (see Tables 4 and 5), the conversion process is energetically more demanding (see Table 1). As a consequence, the electrolysis plant happens to be smaller for LH_2 than for NH_3, reducing, in turns, the cost of the hydrogen generation plant, which appears to have a determinant weight in the TCO.

Additionally, the TCO mapped over the geographical area for each vector is shown in Fig. 13, confirming the trends presented in the previous sections: the HVDC remains the cheapest option followed by GH_2, while NH_3 remains slightly cheaper than LH_2, both still falling behind the non-shipped energy vectors. However, the gap between the shipped and non-shipped energy vectors is notably reduced when onshore storage is not considered in the techno-economic tool.

4.6. Practical considerations

Results obtained from the simulations show that, regardless of the form, green H_2 will have a limited capacity to change the floating offshore wind sector, at least if only economic aspects are considered. On the one hand, the wind resource and, thus, the CF are clearly the determining factors when assessing the economic feasibility of

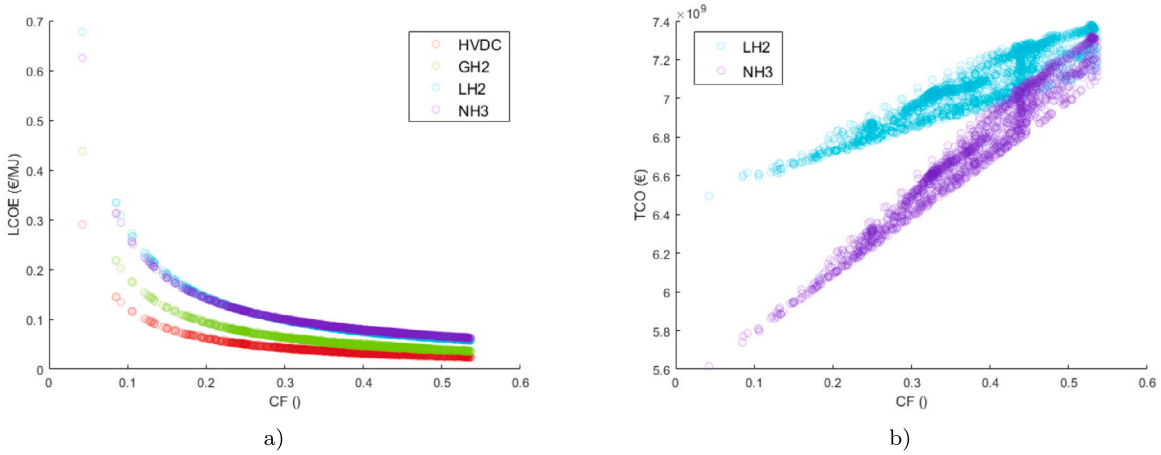

Fig. 12. (a) LCOE of energy vectors without onshore storage, and (b) TCO for LH_2 and NH_3 without onshore storage. HVDC depicted in red, GH_2 in green, LH_2 in blue, and NH_3 in purple.

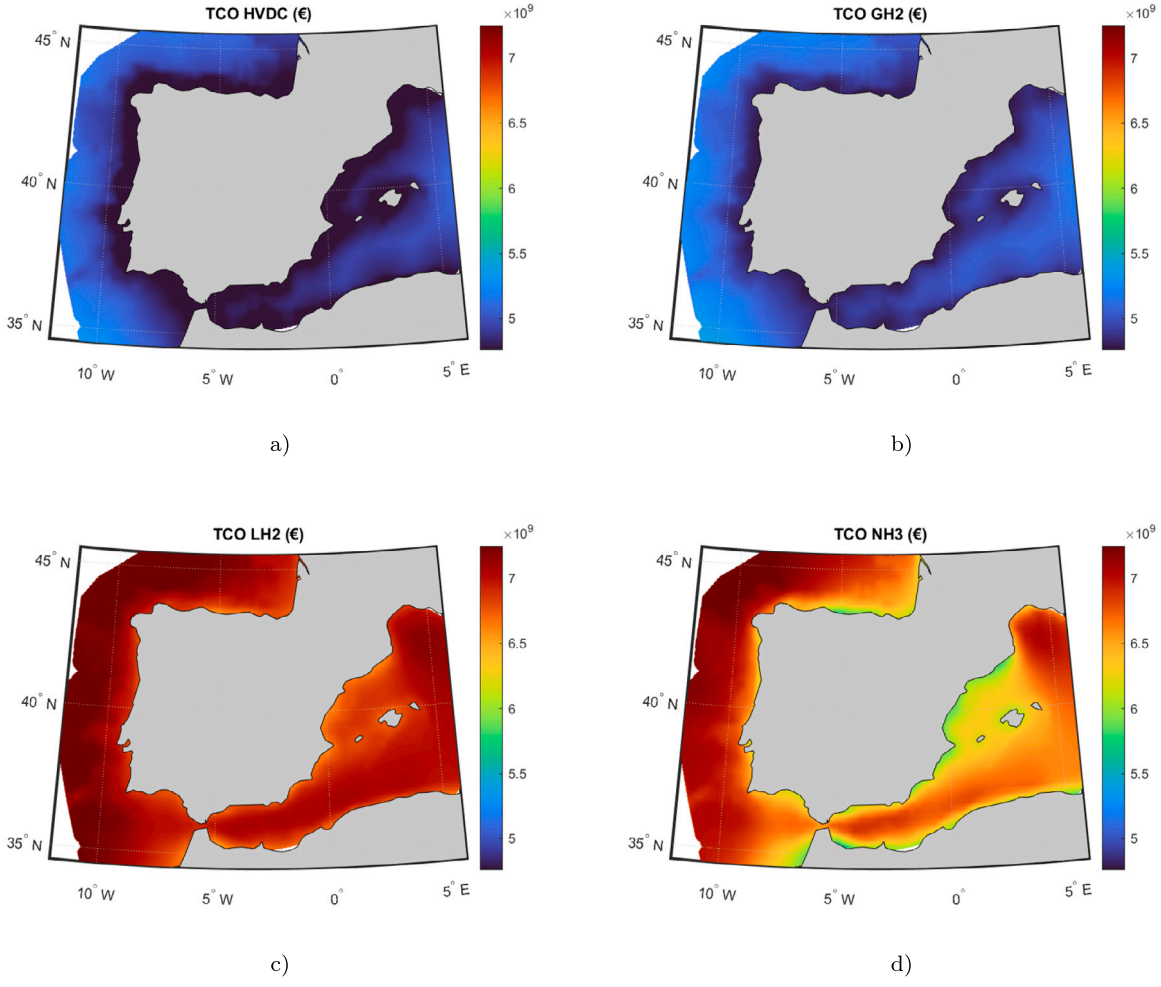

Fig. 13. Total Cost of Ownership without considering onshore storage: (a) HVDC, (b) GH_2, (c) LH_2 and (d) NH_3.

green hydrogen production in floating offshore wind farms. On the other hand, any advantage of the shipped H_2-carrying vectors seems to be very limited in economic terms. Therefore, as long as there are enough available locations with favourable wind conditions close to the shore, the offshore wind sector is expected to focus on building wind farms for electricity generation, integrating electricity into the national grids by means of HVDC cables. Only an exceptional development of H_2-based technologies could encourage future developers to invest in alternative energy vectors in such relatively close-to-shore areas. However, other markets and scenarios may be interesting for the generation of H_2-based vectors: supplying energy to the *in-situ* O&M infrastructure/vessels, reducing the curtailment in offshore farms, and producing energy in locations further offshore, *i.e.* several thousands of kilometres from shore where HVDC may not be technologically feasible. These scenarios are out of the scope of the present paper, but will be analysed in future studies.

In addition, it should be noted that H_2-based energy vectors have been compared to electricity, which is the cheapest energy form nowadays. Nevertheless, as detailed in the introduction, other energy forms are also necessary, which are particularly challenging to substitute by clean sources. As a consequence, the ORE sector should assume that, in near-future, the development of offshore H_2 infrastructures will be oriented towards replacing other non-electrical energy sources. The European Union Hydrogen Strategy already points in this direction, and sets goals of built electrolyser capacity for the coming decades [68]. In fact, H_2 carriers are not only energy vectors, but also end-use products. For example, NH_3 is not only useful as fuel, but it is already used for producing fertilisers. Hydrogen-based fuels are also necessary for uses not appropriate for electrification, and even for supporting the electricity grids as grid scale storage or reserve capacity.

On a shorter term, the first H_2 based vector deployed will probably be GH_2, being a cheaper, simpler and more mature technology. On a longer term, if a specific geographical region becomes saturated with offshore wind farms, the production of shipped vectors could allow the use of a flexible fleets of carrier vessels. These fleets could dynamically change the wind farm from which they receive the energy vectors and the harbours to which they deliver it according to production and demand. This option could also be part of a global trade of renewable energy products.

5. Conclusions

In this study, a holistic techno-economic model is presented for the assessment of green hydrogen(H_2) production from offshore wind farms deployed in far-offshore locations. Apart from the all-electric energy vector, other H_2-carrying energy vectors are considered, such as gas (GH_2) and liquid hydrogen (LH_2), or ammonia (NH_3). To the best of authors' knowledge, this study addresses the limitations observed in prior studies by introducing a single simulation framework that includes and combines (i) realistic wind resource data for the estimation of the energy generation, (ii) realistic port locations to estimate the transport costs, (iii) dynamic effects coming from the variability in the wind resource, (iv) different H_2-based energy vectors and transportation alternatives, and (v) losses in the different conversion stages from electricity to each H_2-based vector. The model has been verified against the literature and applied over a broad area off the Iberian Peninsula. Hence, the three H_2-carrying energy vectors are compared against the all-electric configuration (HVDC). The main conclusions of the study are highlighted below:

- The results indicate that the costs associated with all the considered energy vectors, *i.e.* HVDC, GH_2, LH_2 and NH_3, are consistent with the literature, validating the developed tool for the techno-economic assessment of far-offshore H_2-based projects.
- The available wind resource and, thus, the capacity factor, stand as the most important factors in determining the economic feasibility of H_2 production projects in offshore wind farms. Hence, considering the spatial and temporal variability of the resource for the techno-economic analysis is demonstrated to be relevant. Other apparently relevant factors, such as the bathymetry or the distance to shore/port, have shown a reduced influence on both the total costs (represented by the Total Cost of Ownership) and the levelised expenses (represented by the Levelised Cost of Energy and the Levelised Cost of Energy Vectors).
- For any given site, the all-electric HVDC is always the most economic alternative. Among the studied H_2-carrying energy vectors, GH_2 seems to be the most appealing, providing costs close to HVDC. Indeed, taking into account the economic advantages of different energy vectors and their use on land, offshore produced H_2 could become a favourable choice as long as GH_2 projects including pipelines are technically feasible.
- The shipped vectors (*i.e.* LH_2 and NH_3) always have greater expenses, around two- to three- times greater, rendering them non-competitive at their current level of maturity. Nevertheless, the assumptions considered for onshore storage dimensioning in LH_2 and NH_3 vectors seem too restrictive and may partly cause the observed over-cost of these alternatives. This may result in a biased comparison framework, since the cost of the onshore infrastructure for the integration of the HVDC and GH_2 vectors already exist and, thus, their cost is assigned to external (public) bodies.
- When the cost of onshore storage infrastructure is equally neglected in all the vectors, LH_2 and NH_3 remain as the most expensive H_2-carrying vectors, regardless the simulated location. However, in those sites where the CF is high enough (over 0.4), LH_2 and NH_3 start to be competitive with GH_2 and HVDC. Additionally, in locations with high wind resource conditions, NH_3 projects are observed to become more expensive than LH_2.

All in all, results suggest that, as long as there are enough available locations with favourable wind conditions close to the shore, offshore wind development is expected to focus on building wind farms for electricity generation. Nevertheless, other markets and end-users may be interesting for the consumption of H_2-based vectors, including energy-intensive industries like steelworks; H_2-demanding processes, such as fertiliser production; and offshore farms themselves for supplying auxiliary systems and/or operation and maintenance fleets, and reducing curtailment. In addition, H_2-based vectors can enable the access to far-offshore locations where the connection to shore via HVDC cables may not be technologically feasible. These scenarios are out of the scope of the present paper, but will be analysed in future studies.

CRediT authorship contribution statement

Andoni Gonzalez-Arceo: Conceptualization, Methodology, Software, Visualization, Data curation. **Ricardo Blanco-Aguilera:** Conceptualization, Formal analysis, Methodology, Software, Visualization, Writing – original draft. **Joanes Berasategi:** Formal analysis, Methodology, Writing – review & editing. **Manex Martinez-Agirre:** Formal analysis, Methodology, Writing – review & editing. **Abel Martinez:** Conceptualization, Writing – review & editing. **Gregorio Iglesias:** Conceptualization, Writing – review & editing. **Markel Penalba:** Conceptualization, Data curation, Formal analysis, Funding acquisition, Methodology, Project administration, Visualization, Writing – review & editing.

Declaration of competing interest

The authors declare that they have no known competing financial interests or personal relationships that could have appeared to influence the work reported in this paper.

Data availability

The authors do not have permission to share data.

Acknowledgements

This publication is part of the research project TED2021-132767A-I00 funded by the Spanish Ministry of Science and Innovation, the research project funded by the Basque Government's ELKARTEK 2023 program under the grant No. KK-2023/00051, and the project 2022-CIEN-000052-01 funded by the Gipuzkoa Provincial Council. Finally, the authors from the Fluid Mechanics research group at Mondragon University are also supported by the Basque Government's Research Group Program under the grant No. IT1505-22.

Appendix A. List of harbours

See Table A.1.

Table A.1
List of harbours considered and their coordinates.

Name	Latitude (°)	Longitude (°)
A Coruña	43.36	−8.41
Algeciras	36.13	−5.44
Algiers	36.75	3.06
Alicante	38.35	−0.48
Almería	36.83	−2.46
Aveiro	40.64	−8.65
Barcelona	41.39	2.17
Bejaia	36.76	5.06
Bilbao	43.26	−2.93
Cádiz	36.53	−6.29
Cartagena	37.63	−1.00
Castellón	39.99	−0.05
Denia	38.84	0.11
Figueira da Foz	40.15	−8.86
Gijón	43.54	−5.66
Huelva	37.26	−6.94
Leixoes	41.19	−8.69
Lisbon	38.72	−9.14
Málaga	36.72	−4.42
Marseille Fos	43.39	5.17
Melilla	35.29	−2.94
Oran	35.7	−0.63
Palamós	41.85	3.13
Palma	39.57	2.65
Pasaia	43.32	−1.91
Port-la-Nouvelle	43.02	3.04
Santander	43.46	−3.8
Sines	37.95	−8.87
Tanger Med	35.77	−5.82
Tarragona	41.12	1.24
Valencia	39.45	−0.32
Viana Do Castelo	41.68	−8.81
Vigo	42.24	−8.7

Appendix B. Total Cost of Ownership (TCO)

See Figs. B.1, B.2 and B.3.

Appendix C. Nomenclature

Variables

a_{elec}	P_{elec} to H_2 energy–mass conversion ratio
b_{GH_2}	H_2 to GH_2 mass–energy consumption conversion ratio
b_{LH_2}	H_2 to LH_2 mass–energy consumption conversion ratio
b_{NH_3}	H_2 to NH_3 mass–energy consumption conversion ratio
c_{GH_2}	H_2 to GH_2 mass–mass conversion ratio
c_{LH_2}	H_2 to LH_2 mass–mass conversion ratio
c_{NH_3}	H_2 to NH_3 mass–mass conversion ratio
C_{anch}	Cost of an individual anchor
C_{ch}	Cost of mooring lines
$C_{inst,turb}$	CAPEX costs for the installation of the turbine and the platform
C_{moor}	CAPEX costs for the manufacture of the moorings
C_{tug}	Cost of renting a tugboat
d	Distance to port
h	Water depth of the site
$\dot{m}_{H_2}$	Produced hydrogen mass flow
$\dot{m}_{vector}$	Hydrogen-carrying energy vector mass flow
n_{lin}	Number of mooring lines per turbine
$n_{turbine}$	Number of turbines in the wind farm
$n_{turb,trip}$	Amount of turbines that can be carried per trip
P_{elec}	Electric power consumed by the electrolyser
P_{farm}	Total power of the wind farm
$P_{turbine}$	Power of a turbine
P_{vector}	Electric power consumed by the energy vector specific equipment
T_{inst}	Amount of days to install each turbine and foundation
V_{tug}	Speed of a tugboat
η_{farm}	Efficiency of the wind farm

Abbreviations

CAPEX	Capital Expenditure
CF	Capacity Factor
DECEX	Decommissioning Expenditure
DNV	Det Norske Veritas
FOWT	Floating Offshore Wind Turbine
GH_2	Gaseous Compressed Hydrogen
HV	High Voltage
HVAC	High Voltage Alternating Current
HVDC	High Voltage Direct Current
IEA	International Energy Agency
IRENA	International Renewable Energy Agency
LOHC	Liquid Organic Hydrogen Carrier
LCOE	Levelised Cost of Energy
LCOEV	Levelised Cost of Energy Vector
LHV	Lower Heating Value
NH_3	Ammonia
LH_2	Liquid Hydrogen
O&M	Operation and Maintenance
OPEX	Operational Expenditure
ORE	Offshore Renewable Energies
TCO	Total Cost of Ownership
WEC	Wave Energy Converter

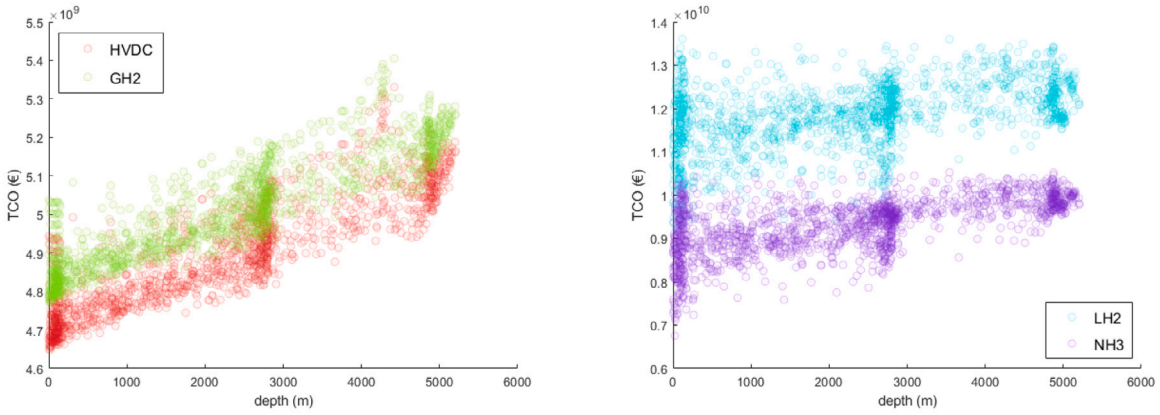

Fig. B.1. Effect of bathymetry in the TCO for (a) HVDC and GH_2, and b) LH_2 and NH_3. HVDC depicted in red, GH_2 in green, LH_2 in blue, and NH_3 in purple.

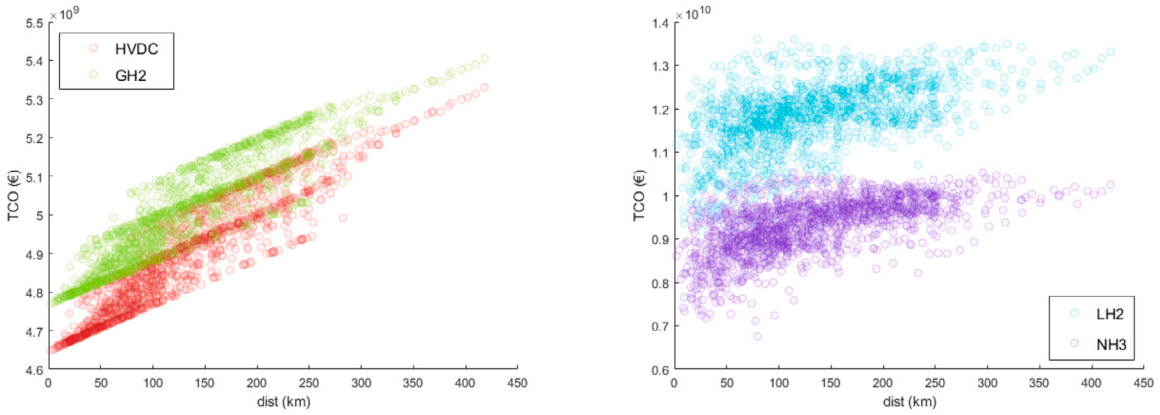

Fig. B.2. Effect of distance to port in the TCO for (a) HVDC and GH_2, and (b) LH_2 and NH_3. HVDC depicted in red, GH_2 in green, LH_2 in blue, and NH_3 in purple.

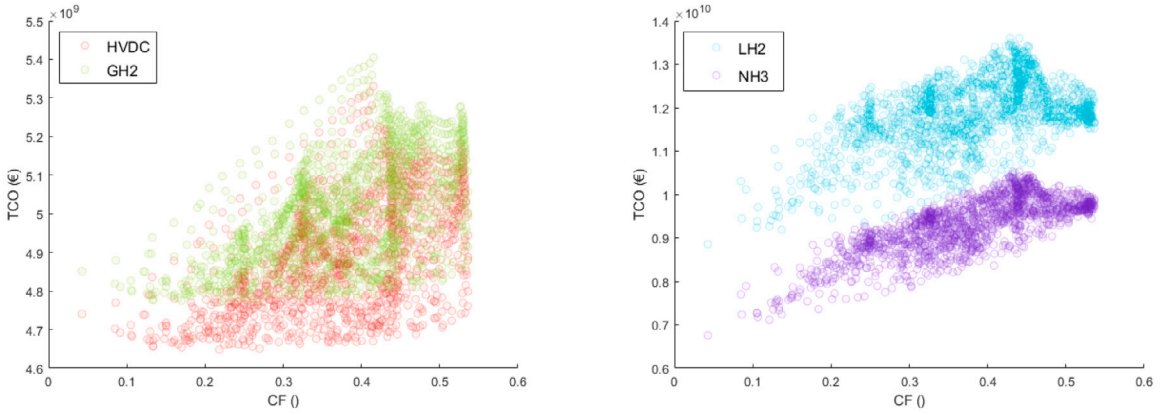

Fig. B.3. Effect of CF in the TCO for (a) HVDC and GH_2, and (b) LH_2 and NH_3. HVDC depicted in red, GH_2 in green, LH_2 in blue, and NH_3 in purple.

References

[1] IRENA. Global energy transformation: A roadmap to 2050. Tech. rep., Abu Dhabi: International Renewable Energy Agency; 2019.

[2] Stéphanie Bouckaert, Pales AF, McGlade C, Remme U, Wanner B. Net zero by 2050: a roadmap for the global energy sector. Tech. rep., Paris: International Energy Agency; 2021, p. 224, URL https://www.iea.org/reports/net-zero-by-2050.

[3] IEA. Renewable heat. renewables 2021. Tech. rep., Paris: International Energy Agency; 2021.

[4] IEA. Hydrogen. Tech. rep., Paris: International Energy Agency; 2022, Available in https://www.iea.org/reports/hydrogen.

[5] IPCC. Global warming of 1.5∘C. Tech. rep., Intergovernmental Panel on Climate Change (IPCC); 2018.

[6] Shin H, Jang D, Lee S, Cho H-S, Kim K-H, Kang S. Techno-economic evaluation of green hydrogen production with low-temperature water electrolysis technologies directly coupled with renewable power sources. Energy Convers Manage

2023;286:117083.
[7] International Energy Agency IEA. World energy outlook 2022. Tech. rep., 2022, URL https://www.iea.org/reports/world-energy-outlook-2022.
[8] IPCC. Mitigation of climate change. working group III contribution to the sixth assessment report of the intergovernmental panel on climate change. Tech. rep., Intergovernmental Panel on Climate Change (IPCC); 2022.
[9] Kakoulaki G, Kougias I, Taylor N, Dolci F, Moya J, Jäger-Waldau A. Green hydrogen in Europe – a regional assessment: Substituting existing production with electrolysis powered by renewables. Energy Convers Manage 2021;228:113649.
[10] International Energy Agency IEA. Global hydrogen review 2022. Tech. rep., 2022, URL https://www.iea.org/reports/global-hydrogen-review-2022.
[11] International Energy Agency IEA. Spain 2021 energy policy review. Tech. rep., 2021, URL https://iea.blob.core.windows.net/assets/2f405ae0-4617-4e16-884c-7956d1945f64/Spain2021.pdf.
[12] DNV. Ocean's future to 2050. Hvik; 2021, Available in https://www.dnv.com/oceansfuture.
[13] Williams R, Zhao F. Global offshore wind report 2023. Tech. rep., Global Wind Energy Council; 2023, URL https://gwec.net/gwecs-global-offshore-wind-report-2023/.
[14] DNV. Floating offshore wind: the next five years. Tech. rep., Det Norske Veritas; 2023, URL https://www.dnv.com/focus-areas/floating-offshore-wind/floating-offshore-wind-the-next-five-years.html.
[15] Martinez A, Iglesias G. Mapping of the levelised cost of energy for floating offshore wind in the European atlantic. Renew Sustain Energy Rev 2022;154:111889.
[16] Crivellari A, Cozzani V. Offshore renewable energy exploitation strategies in remote areas by power-to-gas and power-to-liquid conversion. Int J Hydrogen Energy 2020;45(4):2936–53.
[17] O'Kelly-Lynch PD, Gallagher PD, Borthwick AG, McKeogh EJ, Leahy PG. Offshore conversion of wind power to gaseous fuels: Feasibility study in a depleted gas field. Proc Inst Mech Eng Part A: J Power Energy 2020;234(2):226–36.
[18] Franco BA, Baptista P, Neto RC, Ganilha S. Assessment of offloading pathways for wind-powered offshore hydrogen production: Energy and economic analysis. Appl Energy 2021;286:116553.
[19] Lee J-S, Cherif A, Yoon H-J, Seo S-K, Bae J-E, Shin H-J, et al. Large-scale overseas transportation of hydrogen: Comparative techno-economic and environmental investigation. Renew Sustain Energy Rev 2022;165:112556.
[20] Ebenhoch R, Matha D, Marathe S, Muñoz PC, Molins C. Comparative levelized cost of energy analysis. Energy Procedia 2015;80:108–22.
[21] Colla M, Ioannou A, Falcone G. Critical review of competitiveness indicators for energy projects. Renew Sustain Energy Rev 2020;125:109794.
[22] Astariz S, Iglesias G. Wave energy vs. other energy sources: A reassessment of the economics. Int J Green Energy 2016;13(7):747–55.
[23] Vazquez A, Iglesias G. Grid parity in tidal stream energy projects: An assessment of financial, technological and economic LCOE input parameters. Technol Forecast Soc Change 2016;104:89–101.
[24] Pillai AC, Chick J, Khorasanchi M, Barbouchi S, Johanning L. Application of an offshore wind farm layout optimization methodology at middelgrunden wind farm. Ocean Eng 2017;139:287–97.
[25] Abdelhady S, Borello D, Shaban A. Assessment of levelized cost of electricity of offshore wind energy in Egypt. Wind Eng 2017;41(3):160–73.
[26] Rohan Kumar TS, Stansby PK. Large-scale offshore wind energy installation in northwest India: Assessment of wind resource using weather research and forecasting and levelized cost of energy. Wind Energy 2020;24(2):174–92.
[27] Ohunakin OS, Matthew OJ, Adaramola MS, Atiba OE, Adelekan DS, Aluko OO, et al. Techno-economic assessment of offshore wind energy potential at selected sites in the Gulf of Guinea. Energy Convers Manage 2023;288:117110.
[28] Myhr A, Bjerkseter C, Ågotnes A, Nygaard TA. Levelised cost of energy for offshore floating wind turbines in a lifecycle perspective. Renew Energy 2014;66:714–28.
[29] Lerch M, De-Prada-Gil M, Molins C, Benveniste G. Sensitivity analysis on the levelized cost of energy for floating offshore wind farms. Sustain Energy Technol Assess 2018;30:77–90.
[30] Castro-Santos L, Filgueira-Vizoso A, Carral-Couce L, Formoso JÁF. Economic feasibility of floating offshore wind farms. Energy 2016;112:868–82.
[31] Jiang Y, Huang W, Yang G. Electrolysis plant size optimization and benefit analysis of a far offshore wind-hydrogen system based on information gap decision theory and chance constraints programming. Int J Hydrogen Energy 2022;47(9):5720–32.
[32] Saenz-Aguirre A, Saenz J, Ulazia A, Ibarra-Berastegui G. Optimal strategies of deployment of far offshore co-located wind-wave energy farms. Energy Convers Manage 2022;251:114914.
[33] Dinh QV, Mosadeghi H, Pereira PHT, Leahy PG, et al. A geospatial method for estimating the levelised cost of hydrogen production from offshore wind. Int J Hydrogen Energy 2023.
[34] Giampieri A, Ling-Chin J, Roskilly AP. Techno-economic assessment of offshore wind-to-hydrogen scenarios: A UK case study. Int J Hydrogen Energy 2023.
[35] Kim A, Kim H, Choe C, Lim H. Feasibility of offshore wind turbines for linkage with onshore green hydrogen demands: A comparative economic analysis. Energy Convers Manage 2023;277:116662.
[36] Yan Y, Zhang H, Liao Q, Liang Y, Yan J. Roadmap to hybrid offshore system with hydrogen and power co-generation. Energy Convers Manage 2021;247:114690.
[37] Babarit A, Gilloteaux J-C, Clodic G, Duchet M, Simoneau A, Platzer MF. Techno-economic feasibility of fleets of far offshore hydrogen-producing wind energy converters. Int J Hydrogen Energy 2018;43(15):7266–89.
[38] Singlitico A, Østergaard J, Chatzivasileiadis S. Onshore, offshore or in-turbine electrolysis? Techno-economic overview of alternative integration designs for green hydrogen production into offshore wind power hubs. Renew Sustain Energy Trans 2021;1:100005.
[39] Bonacina CN, Gaskare NB, Valenti G. Assessment of offshore liquid hydrogen production from wind power for ship refueling. Int J Hydrogen Energy 2022;47(2):1279–91.
[40] Guo F, Gao J, Liu H, He P. A hybrid fuzzy investment assessment framework for offshore wind-photovoltaic-hydrogen storage project. J Energy Storage 2022;45:103757.
[41] Jang D, Kim K, Kim K-H, Kang S. Techno-economic analysis and Monte Carlo simulation for green hydrogen production using offshore wind power plant. Energy Convers Manage 2022;263:115695.
[42] Yang B, Liu B, Zhou H, Wang J, Yao W, Wu S, et al. A critical survey of technologies of large offshore wind farm integration: Summary, advances, and perspectives. Prot Control Modern Power Syst 2022;7(1):17.
[43] Elliott D, Bell KR, Finney SJ, Adapa R, Brozio C, Yu J, et al. A comparison of AC and HVDC options for the connection of offshore wind generation in great britain. IEEE Trans Power Deliv 2015;31(2):798–809.
[44] Xiang X, Merlin MM, Green TC. Cost analysis and comparison of HVAC, LFAC and HVDC for offshore wind power connection. IET; 2016.
[45] IRENA. Global hydrogen trade to meet the 1.5° CClimate goal: part II—technology review of hydrogen carriers. United Arab Emirates: IRENA Abhu Dhabi; 2022.
[46] Porté-Agel F, Wu Y-T, Chen C-H. A numerical study of the effects of wind direction on turbine wakes and power losses in a large wind farm. Energies 2013;6(10):5297–313.
[47] Green J, Bowen A, Fingersh LJ, Wan Y-H. Electrical collection and transmission systems for offshore wind power. In: Offshore technology conference. OnePetro; 2007.
[48] Apostolaki-Iosifidou E, Mccormack R, Kempton W, Mccoy P, Ozkan D. Transmission design and analysis for large-scale offshore wind energy development. IEEE Power Energy Technol Syst J 2019;6(1):22–31.
[49] Danish Energy Agency. Technology data for renewable fuels. Energistyrelsen; 2018, URL https://ens.dk/en/our-services/projections-and-models/technology-data/technology-data-renewable-fuels.
[50] Garibaldi L, Blanco-Aguilera R, Berasategi J, Martinez-Agirre M, Giorgi G, Bracco G, et al. Holistic and dynamic mathematical model for the assessment of offshore green hydrogen generation and electrolyser design optimisation. Energy Convers Manage 2023;294:117488.
[51] Dokhani S, Assadi M, Pollet BG. Techno-economic assessment of hydrogen production from seawater. Int J Hydrogen Energy 2023;48(26):9592–608.
[52] European Central Bank. ECB reference exchange rate, US dollar/Euro, 2:15 pm (C.E.T.) - Quick View - ECB Statistical Data Warehouse, URL https://sdw.ecb.europa.eu/quickview.do?SERIES_KEY=120.EXR.D.USD.EUR.SP00.A.
[53] International Energy Agency. Offshore wind outlook 2019 – analysis. IEA, URL https://www.iea.org/reports/offshore-wind-outlook-2019.
[54] Lerch M. Qualification of innovative floating substructures for 10MW Wind turbines and water depths greater than 50m. Tech. rep., Fundació Institut de Recerca en Energia de Catalunya-IREC; 2019, URL https://www.google.com/url?sa=i&url=https%3A%2F%2Fec.europa.eu%2Fresearch%2Fparticipants%2Fdocuments%2FdownloadPublic%3FdocumentIds%3D080166e5c3ac71f4%26appId%3DPPGMS&psig=AOvVaw1ajtqPfzjCbh3nx2Qg9zvh&ust=1699963893280000&source=images&cd=vfe&opi=89978449&ved=2ahUKEwjtlZiR-cCCAxV_uCcCHbQ4D2IQr4kDegQIARB5.
[55] Johnston B, Foley A, Doran J, Littler T. Levelised cost of energy, a challenge for offshore wind. Renew Energy 2020;160:876–85.
[56] Bjerkseter C, Ågotnes A. Levelised costs of energy for offshore floating wind turbine concepts. [Master's thesis], Norwegian University of Life Sciences, Ås; 2013.
[57] Cavazzi S, Dutton A. An offshore wind energy geographic information system (OWE-GIS) for assessment of the UK's offshore wind energy potential. Renew Energy 2016;87:212–28.
[58] International Energy Agency. The future of hydrogen - Seizing today's opportunities. Tech. rep., 2019.
[59] Bortolotti P, Tarres HC, Dykes K, Merz K, Sethuraman L, Verelst D, et al. IEA wind task 37 on systems engineering in wind energy – WP2.1 reference wind turbines. Tech. rep., International Energy Agency; 2019, URL https://www.nrel.gov/docs/fy19osti/73492.pdf.
[60] Vázquez A, Izquierdo U, Enevoldsen P, Andersen F-H, Blanco JM. A macroscale optimal substructure selection for Europe's offshore wind farms. Sustain Energy Technol Assess 2022;53:102768.
[61] Zhang J, Fowai I, Sun K. A glance at offshore wind turbine foundation structures. Brodogradnja: Teorija i praksa brodogradnje i pomorske tehnike 2016;67(2):101–13.

[62] National Geospatial-Intelligence Agency. World port index. Tech. rep., 2023, URL https://msi.nga.mil/Publications/WPI. [Accessed 9 July 2023].
[63] Castro-Santos L, Bento AR, Silva D, Salvação N, Guedes Soares C. Economic feasibility of floating offshore wind farms in the north of Spain. J Mar Sci Eng 2020;8(1):58.
[64] Pacheco A, Gorbeña E, Sequeira C, Jerez S. An evaluation of offshore wind power production by floatable systems: A case study from SW Portugal. Energy 2017;131:239–50.
[65] Musial W, Heimiller D, Beiter P, Scott G, Draxl C. 2016 offshore wind energy resource assessment for the united states. Tech. rep., Golden, CO (United States), National Renewable Energy Lab.(NREL); 2016.
[66] Hersbach H, Bell B, Berrisford P, Hirahara S, Horányi A, Munoz-Sabater J, et al. The era5 global reanalysis. Q J R Meteorol Soc 2020;146(730).
[67] Voormolen J, Junginger H, Van Sark W. Unravelling historical cost developments of offshore wind energy in europe. Energy Policy 2016;88:435–44.
[68] European Comission. A hydrogen strategy for a climate-neutral Europe. 2020, URL https://eur-lex.europa.eu/legal-content/EN/TXT/?uri=CELEX:52020DC0301.